Dissertation
submitted to the combined Faculties for the Natural Sciences and for Mathematics of the Ruperto-Carola University of Heidelberg, Germany
for the degree of
Doctor of Natural Sciences

Presented by
Agnieszka Sadowska
Diploma: Master of Biotechnology, University of Gdansk
Born in Gdansk, Poland

Oral examination:

Genetic studies on functional redundancy between profilin1 and profilin2 in mice and the role of the profilin ligand Mena in neuronal cell function and mouse behavior

Referees: Prof. Dr Jochen Wittbrodt
Prof. Dr Klaus Unsicker

Acknowledgements

I want to thank my supervisor Walter Witke for giving me the possibility to carry on this project in his group.

I would like to express my gratitude Dr Anne Cecile Trillat for teaching me the methodology used for neuronal cultures and showing an incredible passion for neuroscience. Thank you Cecile for your support to the whole idea as well as for your critical eye looking at my results and their interpretation, but above all for your presence.

I would like to thank the members of The Phenotyping Core Facility, EMBL Monterotondo Karin Gale and Janice Carter help in Phenotyping Analysis of the Mena KO mice.

I would like to thank Pietro Pilo Boyl for involvement in teaching me what is the perfection and for critical comments and discussions on this thesis. Grazie Pietro.

I would like to than Jakky Kelly-Barrett for the injection of my ES cells and generation two of my knock-in mice.

I would love to thank all the members of the Witke group, those with whom I have started in EMBL: James Sutherlad, wonderful friend and teacher, Laura Spinardi for being always next to me, Ralph Gareus for help and critics, Alessia Di Nardo for her Profilin2 KO mice, and all the present members: Christine, Denise, Ekaterina and Emerald who were making my time at the bench enjoyable.

In addition I would like to thank Craig and Mark for making me always laugh and for being present in emergency situations.

And most importantly I would love to thank my boyfriend Claudio for his patience and love, my parents and my sister Edyta that were always ready to listen to me and my friends Magda, Xenka and Aga with whom I could share this experience.

Table of contents

Abbreviations

[(Ca^{2+})i]	intracellular calcium ion
3'UTR	3' untranslated region
5'UTR	5' untranslated region
aa	amino acid
ADF	actin depolymerizing factor
ANOVA	analysis of variance
ATP	adenosine 5'-triphosphate
BSA	bovine serum albumine
Ca^{2+}	calcium ion
cDNA	complementary deoxyribonucleic acid
DNA	desoxyribonucleic acid
dNTPs	deoxyribonucleotides
DTT	dithiothreitol
EDTA	ethylenediaminotetraacetate
EGTA	ethyleneglycole-bis[β-aminoethyl ether]-N,N,N',N'-tetraacetate
EVH1	Ena/VASP homology domain1
EVH2	Ena/VASP homology domain2
F-actin	filamentous actin
FCS	fetal calf serum
G-actin	globular actin
GTP	guanosine 5'-triphosphate
HEPES	N-2-hydroxyethylpiperazine-N'-2-ethane sulfonic acid
IPTG	isopropylthio-β-D-galactoside
kb	kilobase
kDa	kilodalton
LB	Lauria-Bertani medium
mRNA	messenger RNA
MTS	3-(4,5-dimethylthiazol-2-yl)-5-(3-carboxymethoxyphenyl)-2-(4-sulphophenyil)-2H tetrazolium, inner salt
NMDA	N-methyl-D-aspartate
PAGE	polyacrilamide - gel electrophoresis
PBS	phosphate buffered saline
PCR	polymerase chain reaction
PH	pleckstrin homology domain
PIP_2	phosphatidylinositol-4,5-bis phosphate
PLP	poly-L-proline
RNA	ribonucleic acid
RT	room temperature
SDS	sodium dodecylsulphate
X-GAL	5-bromo-4-chloro-3-indolyl-β-D-galactoside

List of figures and tables

Summary

Profilin1 and profilin2 are two actin-binding proteins. Biochemically, proflin1 and profilin2 are similar in respect to their interactions with actin, phosphatidylinositol-4,5-bisphosphate (PIP_2), and proteins containing poly-L-proline rich motives among which the Ena/VASP protein family members such as Mena. While profilin1 is highly expressed throughout development and adulthood in most tissues including brain, profilin2 is the neuronal specific isoform. Lack of profilin1 results in early embryonic lethality, while profilin2 KO mice are viable and show behavioral abnormalities.
In this thesis I aimed to address three major questions:

1. Is there functional redundancy between profilin1 and profilin2 *in vivo*?
2. What is the role of the profilin ligand Mena in neuronal cell function and mouse behavior?
3. Is there a common functional pathway for profilin2 and Mena?

In order to address functional redundancy between profilin1 and 2 I generated two different knock-in mouse lines in which profilin1 was substituted by mouse profilin2. However, for unknown reasons expression of profilin2 from the transgene was not detectable in tissues isolated from mice targeted with both knock-in strategies.

My studies on Mena KO mice suggested an involvement of this protein in re-organization of the actin cytoskeleton and axon path-finding. In hippocampal neurons isolated from Mena KO mice, I showed that Mena is normally inhibiting the outgrowth of dendritic processes and cell spreading. In the mutant animals these alterations lead to axonal path-finding defects and behavioral abnormalities. My behavioral analysis showed that lack of Mena leads to impairment of locomotor activity, motor coordination and balance as well as to alteration in stress response. The severity of the phenotype was found to be age-dependent.

Since Mena and profilin2 are known to interact *in vitro* I tried to investigate if both proteins act in common physiological pathways. Therefore, I compared the neuronal cell phenotype and the behavior of Mena KO and profilin2 KO mice. Interestingly, the morphological alterations are very similar in hippocampal neurons from Mena KO and profilin2 KO mice (longer primary processes and faster spreading). In terms of behavior, both KO lines showed alterations in locomotor activity, impairments in motor coordination and balance as well as altered stress response. The overlap and the differences of phenotypes suggest that profilin2 and Mena are linked in common functional pathways, but also that Mena and profilin2 have unique functions in mouse brain physiology.

1. Introduction

Profilins

Cells undergo continuous changes in shape and motility. These processes are initiated in response to either external or internal stimuli and accomplished by the cytoskeleton. In particular the microfilament cytoskeleton is considered to be a highly sensitive recipient of messages conveyed by various signaling pathways. In response to such information the three-dimensional organization of the actin cytoskeleton or the equilibrium between actin filaments and the monomeric actin pool undergoes continuous changes. These events are spatially and temporally controlled.

Two decades ago Carlsson and co-workers discovered profilin, a small 12-16 kDa protein that directly interacts with actin, acidic phospholipids and several other proteins involved in various signal transduction pathways. Since then profilin was identified in all Eukaryotes investigated, such as Protozoa, echinodermata, insects, plants and mammals. Even Vaccinia virus contains a profilin like gene (Blasco et al. 1991). In yeast and Drosophila one profilin gene is expressed while, Arabidopsis, Acanthamoeba, Dictyostelium, Physarum, and plants encode more than one profilin isoform on distinct genes. It was long believed that mammalian species contain only one profilin isoform, however during the execution of a random human cDNA cloning project, a second profilin gene - profilin2 was discovered. To date three profilin isoforms have been identified in mammals. Mouse profilins are encoded on three different genes and called profilin1, profilin2 and profilin3.

The amino acid sequence identity between two isoforms within any given organism is between 54% and 83%; for example, the human profilin1 and profilin2

are 65% identical at the amino acid level but only 35% identical to profilins from lower eukaryotes and about 20% identical to plant profilins. In spite of the considerable degree of sequence variation between profilins from different species, their biochemical properties have been extremely well conserved throughout evolution (Lambrechts et al. 1997). It has been shown that plant and bovine profilin is able to rescue the defects in cell shape, cytokinesis and development that were observed in Dictyostelium profilin null mutant (Karakesisoglou et al. 1996; Schluter et al. 1998).

Biochemical features of profilins

Biochemically, profilin was identified by its ability to bind to poly-L-proline stretches and was shown to form a 1:1 complex with monomeric G-actin (Carlsson et al. 1977). The formation of this complex might represent a mechanism to sequester G-actin from the free cellular pool, although upon binding to actin monomers, profilin *in vitro* increases the rate of nucleotide exchange on the actin monomer, thereby charging the monomer with ATP, and possibly enhancing actin filament dynamics (Goldschmidt-Clermont et al. 1992). *In vitro* data show that profilin does not solely act as a sequestering protein for G-actin. Kinetics studies of actin polymerization have shown that profilin can accelerate actin filament growth if free barbed filament ends are available (Pantaloni and Carlier 1993). This finding suggests that *in vivo* profilin might actually promote actin polymerization.

The only known physiological compounds able to release actin from the profilin-actin complex are the phosphoinositides, especially phosphatidylinositol-4,5-bisphosphate (PIP_2), since the domains responsible for profilin interaction with actin and PIP_2 overlap (Lassing and Lindberg 1985). Profilin binds PIP_2 with high affinity and is able to inhibit the non-tyrosine-phosphorylated form of phospholipase C-γ, suggesting that profilin may also play a role in signal

transduction through tyrosine kinases and phospholipids (Goldschmidt-Clermont et al. 1991). In addition, the profilin-actin complex *in vitro* binds with high affinity to poly-L-proline stretches, suggesting that *in vivo* profilin might bind to proline rich proteins. This property could serve other functions depending on the ligand. The Arp2/3 complex (Machesky et al. 1994), Ena/VASP family members (Reinhard et al. 1995; Gertler et al. 1996), gephyrin (Mammoto et al. 1998), Diaphanous (Watanabe, 1997) and dynamin (Damke et al. 1994) have been shown to interact with profilins. The profilin ligands appear to play a role in the control of cell motility and actin dynamics such as fibroblast migration as well as axon guidance or platelet activation (Aszodi et al. 1999; Lanier et al. 1999; Bear et al. 2002; Loureiro et al. 2002). They were found concentrated at the leading edge of cells suggesting a role in regulating the dynamics of the major protrusive actin structures: lammelipodia thin membrane sheets and membrane spikes known as filopodia (Rottger et al. 1999).

The role of profilin in actin-based motility

Many studies on profilin role in actin - based motility were taking advantage of intracellular pathogens. Certain intracellular pathogenic bacteria such as *Shigella flexneri, Listeria monocytogenes, Rikettsia conorii* as well as an enveloped virus, *Vaccinia virus* (Cudmore et al. 1995), use actin-based motility for their intra- and intercellular movement. Intracellular movement is strictly coupled to a polarized actin polymerization process at one end of the bacterium, resulting in the formation of an actin comet tail or rocket tail. Specific bacterial surface proteins have been identified to be involved in this movement for example VirG or IcsA for *S. flexneri,* and ActA for *L. monocytogenes* (Bernardini et al. 1989). These proteins are anchored in the bacterial membrane, transversely to the peptidoglycan layer, and have an intracellular domain, which recruits cellular

proteins like F-Actin, Arp2/3 complex, N-WASP, actin depolimerizing factor (ADF or cofilin) and capping proteins. Profilin is recruited to sites of active cytoskeletal assembly through the association with N-WASP, a signaling protein that links multiple signaling components to direct actin-dependent events (Suetsugu et al. 1998). In addition, profilin associates with the Arp2/3 complex (Mullins et al. 1998), which is present in lammelipodia and other dynamic, actin-based structures (Machesky et al. 1997) and appears to initiate actin polymerization during the intracellular motility of the pathogenic bacterium *Listeria monocytogenes* (Reinhard et al. 1995; Welch et al. 1997). Profilin also interacts with members of the Ena/VASP protein family, including VASP - Vasodilator-Stimulated Phosphoprotein - (Reinhard et al. 1995) and Mena - mammalian Enabled - (Gertler et al. 1996). Like the Arp2/3 complex, VASP and Mena are recruited by the *Listeria* protein ActA to sites of actin polymerization, where they colocalize with profilin (Theriot and Mitchison 1993; Gertler et al. 1996; Niebuhr et al. 1997). Inhibiting profilin binding to VASP (Kang et al. 1997) or VASP binding to ActA (Smith et al. 1996) impairs *Listeria* motility, suggesting a role of profilin in accelerating the actin-dependent motility of the pathogen.

Apart from pathogen motility, profilin has been shown to be important for motility of eukaryotic cells. For example, *D. discoideum* mutants deficient for profilin show defects in F-actin content, cytokinesis and development (Haugwitz et al. 1994). Yeast lacking profilin show defects in cell shape and actin localization (Haarer et al. 1990). Actin cables are no longer visible, the polarity of the cells is lost, and the normal axial budding of haploid cells becomes random. In *Drosophila,* genomic deletions of the *chickadee* locus (*Drosophila* profilin) resulted in a late embryonic lethal phenotype indicating that profilin is essential for fly development. Lack of profilin during *Drosophila* oogenesis leads to a failure in proper assembly of nurse cell actin filament bundles and abnormal mitosis (Cooley et al. 1992; Manseau et al. 1996). Using an RNA interference approach (RNAi) in *C. elegans* it was shown that profilin PFN-1 is required for assembly and stability of the cortical

actomyosin cytoskeleton as well as for oogenesis and fertilization (Karakesisoglou et al. 2000).

Profilins in mouse

To date, three profilins profilin1, 2 and 3 were identified in mouse, each encoded on a distinct gene (Kwiatkowski and Bruns 1988; Honore et al. 1993; Braun et al. 2002). Profilin1 is highly expressed in most tissues except skeletal muscle, while profilin2 is present predominantly in neuronal tissues and at lower levels in uterus and kidney (Witke et al. 1998). Two spliced variants of profilin2 profilin2A and profilin2B have been identified (Di Nardo et al. 2000). Since profilin2A is the main brain specific profilin2 isosform in mice, I will simply refer to profilin2A as profilin2 in following work. Recently a novel profilin isoform, profilin3, was detected in mouse, rat and human tissues (Hu et al. 2001; Braun et al. 2002). Mouse profilin3 expression is a testis specific isoform (Braun et al. 2002).

During embryonic development profilin1 is expressed highly at all stages including embryonic stem (ES) cells. Profilin2 is expressed at very low level in ES cells and in early embryos, with peak expression around day E13. The increase in the expression level correlates with rapid brain development around E13.

Mouse profilin1 and profilin2 share 62% identity at the amino acid level. The biochemical properties of these two profilin isoforms are very similar with respect to actin binding, PIP_2 binding and affinity for poly-L-proline (Gieselmann et al. 1995; Lambrechts et al. 1995).

Role of profilin1 and profilin2 in mice

The functional differences between profilin isoforms are not yet known and their role may be dependent on the tissue specific expression, on the total intracellular concentration of the protein or on the specific complexes formed with their ligands. In order to study the role of mouse profilins *in vivo* conventional profilin1 and profilin2 knockout mice were generated in our laboratory.

Mutation of the profilin1 gene leads to an embryonic lethal phenotype: KO embryos die before implantation probably from defects in cytokinesis (Witke et al. 2001). Heterozygous mice for profilin1, which express 50% of profilin1, are viable and have a normal longevity.

Profilin2 deficient mice are viable and show normal brain anatomy. Profilin2 KO hippocampal neurons spread fasted after plating and produce longer dendritic processes. Profilin2 mutant mice show behavioral abnormalities, such as impaired maternal behavior, altered stress response and hyperactivity (Di Nardo, PhD thesis, Pilo Boyl unpublished data).

Profilin1 and profilin2 are both expressed in mouse brain

In the mouse brain the expression level of profilin2 is three times higher compared to the expression of profilin1. Because in brain both profilins are expressed, this tissue serves as an ideal model to study the general functions of profilins as well as specific activities of profilin2 (Witke et al. 2001). Using MALDI mass spectrometry protein complexes formed by profilin1 and profilin2 were identified (Witke et al. 1998). Interestingly, these complexes were very different from each other and different from the ones described in lower eukaryotes (Machesky et al. 1994). The components of profilin complexes are involved in signal transduction, endocytosis and synaptic recycling. The major components of the profilin1 complex in mouse brain are: clathrin, valosine containing protein

(VCP), hsp70 and actin. The most prominent component of profilin2 complex is dynamin1, a protein known to be involved in clathrin-mediated vesicle formation (Damke et al. 1994). In primary mouse hippocampal neurons profilin2 and dynamin1 co-localize at vesicular structures, supporting the idea that the profilin2 complexes exist *in vivo* and might play a role in vesicle recycling (Witke et al. 1998). Synapsin1A/B, synapsin2A/B, ROCK2 a downstream effector of Rho signaling pathway, and Mena were detected as other abundant components of profilin2 complex in the mouse brain. Mena has been shown to have an important function in regulating cytoskeletal dynamics and recent work has suggested that Mena might link profilin to this process. Table1 summarizes the proteins detected in profilin1 and profilin2 brain complexes.

Profilin1 complex	Profilin2 complex
Actin	Actin
Tubulin	ROCK2
clathrin	POP
Hsp 70	HEM
Mena, VASP	Dynamin1
VCP	Synapsin1A/B
	Synapsin2A/B
	Hsp70
	Mena,VASP

Table1 List of proteins detected in profilin1 and profilin2 protein complexes by MALDI mass spectroscopy and western blot in the mouse brain.

Mena, a member of the Ena/VASP protein family, and its interaction with profilins

An important question was raised by the biochemical data on profilin complexes and the *in vivo* findings in the KO mice, whether the specific complexes account for the different phenotype of the mutant mice. In this respect, the observations made in the double mutant for profilin1 and the ligand Mena is particularly informative. The brains of Mena KO mice exhibit striking abnormalities in the corpus callosum and hippocampal commissure. Fibers in the corpus callosum fail to project medially and to cross the midline, therefore there is no proper connection formed between the two hemispheres (Lanier et al. 1999). The failure of Mena-deficient growth cones to choose the correct path suggests that Mena has a role in growth cone's ability to read or respond adequately to the guidance cues.

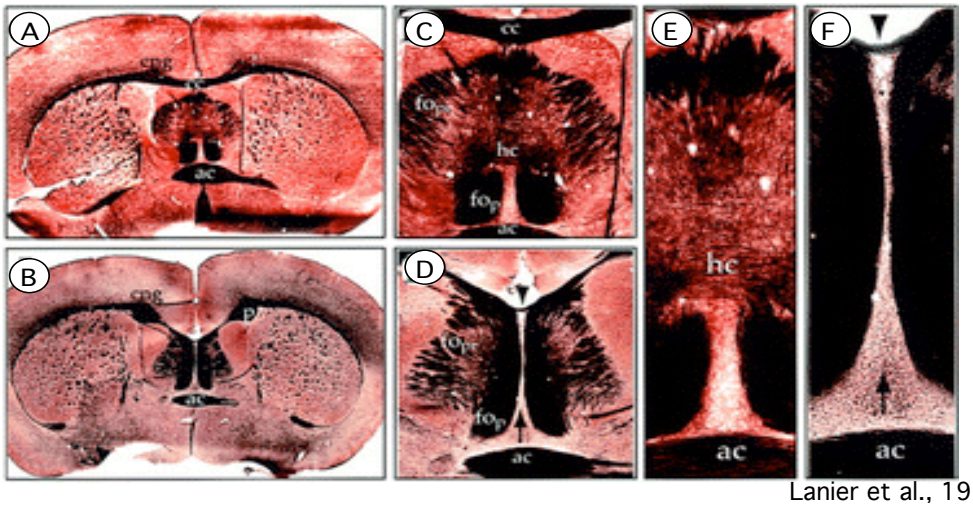

Lanier et al., 1999

Figure 1 Histological comparison of WT and Mena KO adult brains
Matched section of WT and Mena KO brains were analyzed by silver staining.
(A,C,E) Coronal section through wild type (WT) brain, where structures of pre- and post commissural fornix (fopr and fop, respectively) and the hippocampal commissure (hc) are shown.
(B,D,F) In Mena KO brains many of the above structures are abnormal or missing.
(D and F) A few fibers from the corpus callosum appear to project ventrally and cross just above the dorsal fornix (arrow head).
(D and F) Cells are visible in the midline (arrow), but fibers of the hippocampal commissure do not appear to cross as they do in the wild type control (compared to C and E)

Mice heterozygous for profilin1 gene and deficient for Mena expression die prenatally from cephalic tube closure defects. This suggests the existence of a common pathway where the two proteins are acting (Lanier et al. 1999).

The Ena/VASP protein family is a structurally conserved family found in vertebrates, invertebrates and *Dictyostelium.* This family is composed of *Drosophila Enabled* (Ena), *C. elegans* UNC-34/Enabled, vertebrate EVL (Ena/VASP-like protein), VASP and Mena. Ena/VASP proteins are implicated in cell motility (Bear et al. 2000; Goh et al. 2002). Mena and all the other Ena/VASP proteins share a highly conserved tripartite structure: a proline rich core flanked by two defined regions called Ena/VASP homology domains 1 and 2, EVH1 and EVH2 (Figure 2).

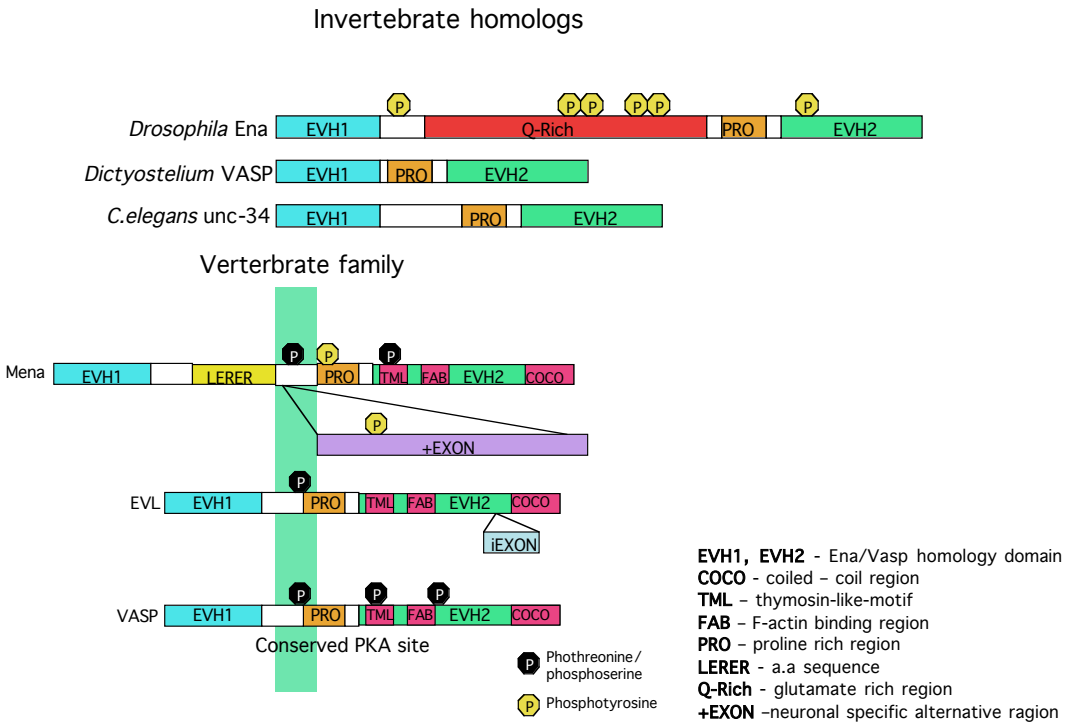

Figure 2 Representation of the structural organization of the highly related vertebrate proteins Mena, VASP and EVL and their invertebrate orthologs: Ena, VASP and UNC-34.
All members share a conserved domain structure: PRO, a proline rich core, flanked by two distinct regions called Ena/VASP like domain (EVH1 and EVH2). All verterbrate family members are substrates for Ser/Thr protein kinase A and G. Ena is a substrate for Abl tyrosine kinase and contains six phosphorylation sites.

The N-terminal EVH1 domain binds directly to a consensus motif and plays an essential role in targeting Ena/VASP proteins to focal adhesion sites, while the central proline-rich region serves as a docking site for several SH3 (Src-homology 3) and WW domain-containing proteins like Abl, IRSp53 and FE65 as well as for profilin (Lambrechts et al. 2000). The EVH2 domain is required for oligomerization (Bachmann et al. 1999) and binding of actin (Bachmann et al. 1999; Walders-Harbeck et al. 2002). In fibroblasts, Ena/VASP proteins regulate the protrusive step of motility by controlling the geometry of actin networks within lamellipodia (Bear et al. 2002). However, these findings seem to contradict the enhanced intracellular actin based motility of *L. monocytogenes* caused by presence of Ena/VASP and profilin (Loisel et al. 1999; Grenklo et al. 2003). Since distinct regions within the Ena/VASP molecule are required for lammelipodial protrusion of fibroblasts and *Listeria* motility, the observed paradox might be explained by the different functions performed by the Ena/VASP proteins in these two actin-dependent processes. Ena/VASP proteins are also implicated in many other actin-dependent processes, including axon guidance (Gertler et al. 1990), neural tube closure (Lanier et al., 1999), attenuation of platelet aggregation (Aszodi et al. 1999), T-cell activation, phagocytosis (Krause et al. 2000), cell–cell adhesion and the intracellular movement of the bacterial pathogen *L. monocytogenes* (Vasioukihin et al., 2001).

EVH1 domain. The structure of EVH1 domain of Ena/VASP has been solved and has revealed a direct binding to the consensus motif (D/E)-FPPPP-X(D/E)(D/E) (Niebuhr et al. 1997). This recognition sequence is identified in a number of cellular proteins, which preferentially localize at focal adhesion sites. The interaction of Ena/VASP through EVH1 domain is confirmed for the cytoskeletal proteins zyxin and vinculin (Beckerle 1997) as well as for the transmembrane axon guidance molecules Robo (Godenschwege et al. 2002) and Semaphorin6A-1 (Klostermann et al. 2000). The EVH1 domain of Ena/VASP proteins is involved in the association of Mena and VASP with sites of an actin tail assembly on *L.*

monocytogenes surface by direct binding to proline-rich motifs of the bacterial ActA protein. This binding would stimulate intracellular movement of *Listeria* (Smith et al. 1996).

The proline rich region (PRO region) of Ena/VASP proteins contains binding sites for profilin and SH3 and WW domain-containing proteins. Deletion of this region has no effect on the ability of Ena/Vasp proteins to localize and to support normal rates of fibroblast movement. This indicates that this region is not essential for the function of Ena/VASP within lammelipodia during this type of motility. However, the PRO region, by interaction with profilin, recruits profilin-actin complexes to rapidly assemble the actin tail during *Listeria* movement and lack of the PRO region in Ena/VASP proteins reduces speed of *L. monocytogenes.* Considering the genetic interaction between Ena and Abl in *Drosophila* (Gertler et al. 1990) it is possible that the physical interaction between the PRO region and the SH3 domain of Abl kinase may play a role in connecting Abl signaling to Ena/VASP protein function. Also *Dictyostelium* mutagenesis studies revealed an important role of the PRO region in filopodia formation, suggesting its requirement for initiation or stability of these structures.

EVH2 domain. The EVH2 domain is composed of three conserved regions: a G-actin binding region known as thymosin-like-motif (TML), an F-actin binding region (FAB) and a coiled-coil region (COCO). In addition, phosphorylation sites for PKA/PKG kinases were found within EVH2 domains of Mena, VASP and EVL. Deletion of the TML region leads to cellular miss-localization of the Ena/VASP proteins and their diffused distribution throughout the cytoplasm and weak detection in the focal adhesions as well as along the leading edge of lammelipodia. The FAB region binds to F-actin and plays a crucial role in targeting Ena/VASP proteins to the leading edge. The FAB is also involved in proper regulation of cell motility possibly by maintaining the anti-capping activity of Ena/VASP proteins (Bear et al. 2002). The C terminus region of EVH2 domain contains the coiled-coil motif that mediates oligomerization of Ena/VASP proteins (Bachmann et al.

1999), which seems to be important for *in vitro* actin nucleation and the binding to various Ena/VASP ligands.

Ena/VASP proteins regulate axonal outgrowth

Actin - based motility is critical for neuronal development and neural crest cell migration. Genetic studies performed on several models revealed that Ena/VASP proteins are required for normal axon pathfinding. In wild-type *Drosophila*, the intersegmental nerve group b (ISNb) subset of motor axons defasciculate from the intersegmental nerve just adjacent to the ventral nerve cord and innervate their target muscles (Vactor et al. 1993). In Ena mutant flies, the ISNb neurons ignore the signals to turn and normally innervate their muscle targets and instead continue processing dorsally (Wills et al. 1999). In *C. elegans*, mutation in UNC-34/Ena gene leads to misguidance of the motor axons and premature termination of axons in the ventral nerve cord (Yu et al., 2002).

Goals of my PhD thesis

Biochemical similarities of profilins with respect to actin, PIP_2 and poly-L-proline binding as well as rescue experiments performed on *Dictyostelium* mutants lacking profilin using plant and bovine profilins (Karakesisoglou et al. 1996; Schluter et al. 1998) have led to hypothesize a functional redundancy between profilin1 and profilin2 genes in mice. Due to the importance of this question the first part of my PhD thesis was aimed at addressing a possible *in vivo* functional redundancy between profilin1 and profilin2. For this purpose I performed a study where profilin1 was substituted by profilin2 in mice. Considering the dramatically different phenotypes shown by the two KO mice for profilin1 and profilin2, which

might be due to differences in developmental expression pattern, tissue distribution as well as subcellular localization, this approach would have addressed the biochemical functional redundancy between the two proteins as well as their functional specificity.

In the second part of my thesis I focused on the consequences of Mena gene inactivation on neuronal cell development and behavior. Therefore, I analyzed the morphology of Mena KO hippocampal neurons and tested the behavior of Mena KO mice.

In the last part, I was interested in possible common pathways for profilin2 and Mena *in vivo.* In order to address this issue I compared the neuronal cell phenotype and the behavior of profilin2 and Mena KO mice.

2. Results

2.1 Functional redundancy between profilin1 and profilin2 in mice

Studies on tissue distribution and developmental expression of profilin1 and profilin2 as well as similarities with respect to their interactions with actin, phosphoinositides (PIP_2) and poly-L-proline rich motives suggest the possibility of functional redundancy between the two genes. In order to address this question, I decided to replace profilin1 by profilin2 *in vivo.* The mouse model generated was meant to express profilin2 in all the tissues that normally express profilin1.

2.1.1 Conditional replacement of the mouse profilin1 gene by the human profilin1/mouse profilin2 (IRES-hP1/mP2) cassette

In order to replace profilin1 by profilin2 *in vivo,* the targeting construct that carries the human profilin1/mouse profilin2 cassette was generated as described in (4.1.1). Human and mouse profilin1 share 98% identity in amino acid sequence and similar affinity for actin, PIP_2, poly-L-proline stretches. The availability of a specific antibody against human profilin1 (2H11) allowed me to easily identify the functionality of the knock-in allele. Translation of the hP1/mP2 from the knock-in allele is controlled by an IRES (Internal Ribosome Entry Site) sequence. Due to the design of the targeting construct, transcription results in a mRNA composed of human profilin1 and mouse profilin2 followed by the BGH 3'UTR and polyadenylation signal. The expression of mouse profilin2 is achieved only after conditional removal of hP1. The NEO resistance cassette can be removed upon FLP

induced recombination (4.1.3). The final targeting construct contained a 0.7 kb short homology arm and a 3.8 kb long homology arm for the recombination in the genomic locus of mouse profilin1, as shown in Figure 3A. ES cells were electoporated as described with the linearized targeting vector (4.1.1; 4.2.2a). After selection, 143 clones were picked, expanded, and genomic DNA prepared. The clones were tested by Southern blot using *Hind*III digest and the external *Nco*I/*Bam*HI probe, as shown in Figure 3A. A band of 10 kb was expected from the wild type allele and a band of 8.7 kb in case of an homologous recombination event due to the presence of a new *Hind*III site introduced together with the human profilin1 coding sequence. Four ES cell clones showed the right pattern for homologous recombination (Figure 3B). Single copy integration was subsequently confirmed using a neomycin probe (data not shown).

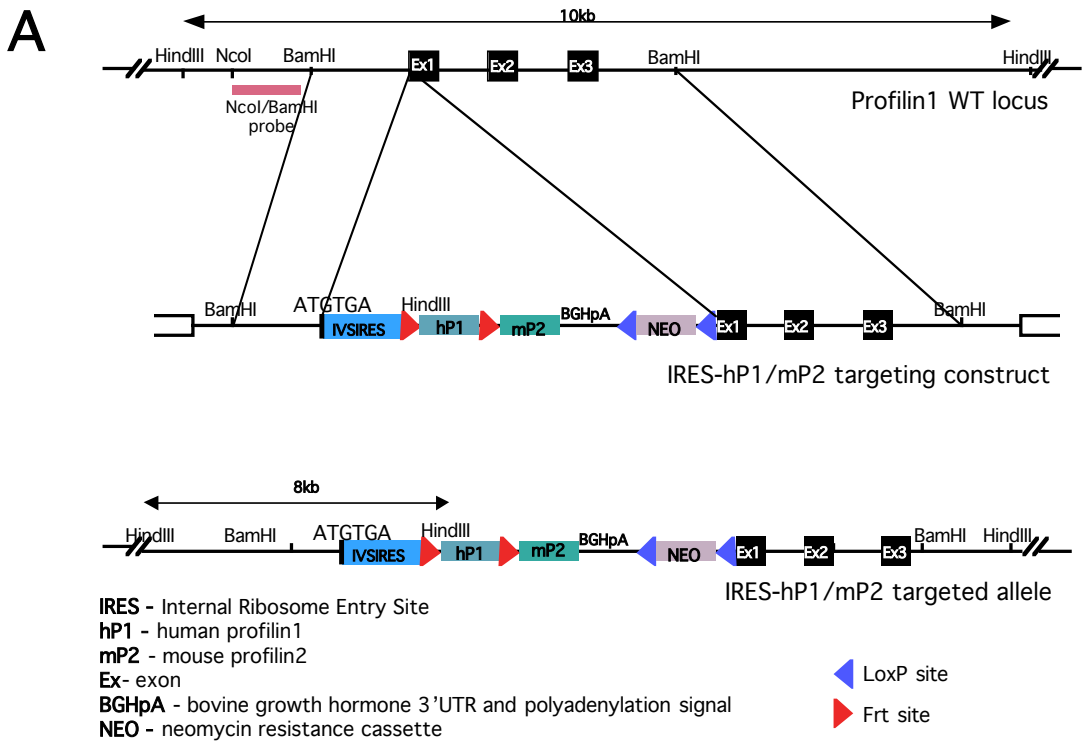

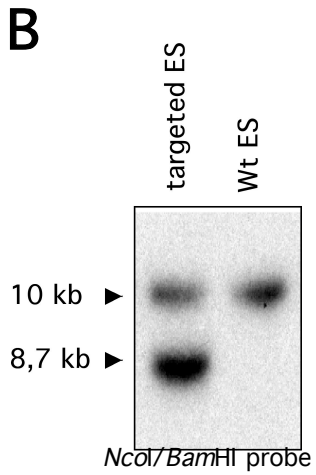

Figure 3 Strategy used for the replacement of profilin1 by the IRES-hP1/mP2 allele.

A) Schematic drawing representing the organization of the wild type locus of mouse profilin1, the targeting construct and the targeted allele. The genomic regions for homologous recombination are 0.7kb (left arm) and 3.8kb (right arm).

B) Southern blot analysis of genomic DNA from a targeted and a wild type ES cell clone digested with *Hind*III. With the external *Ncol/Bam*HI probe the expected 8.7kb band for homologous recombinats was identified.

2.1.2 Generation of the IRES-hP1/mP2 knock-in mouse

One targeted ES cell clone (#50) was injected into C57 blastocysts, and four chimeras were generated. After intercrosses performed between chimeras and wild type C57 famales, agouti coat color mice were obtained indicating that germline transmission had occured. Agouti offspring were genotyped by PCR amplification of human profilin1 and the NEO genes using specific pairs of primers as shown in Figure 4.

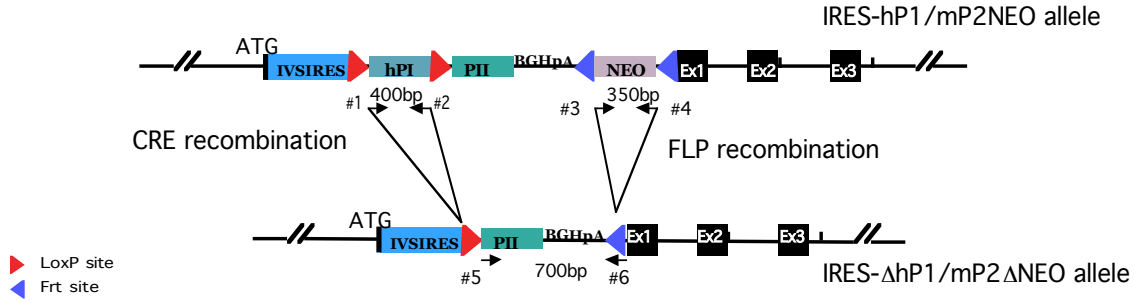

Figure 4 Schematic drawing of the PCR strategy used for screening of the IRES-hP1/mP2 knock-in mice.

The localization of specific primer pairs is illustrated. Primers #1 and #2 amplify the hP1 cDNA, primers #3 and #4 amplify a fragment of the NEO resistance cassette and primers #5 and #6 serve for mP2-BGHpA amplification after the FLP recombination (4.1.3). While the amplification of hP1 and the NEO fragment confirms transmission of the knock-in allele, the presence of the mP2-BGHpA band is specific for the deletion of the NEO cassette in the knock-in allele.

2.1.3 Profilin2 expression from the IRES-hP1/mP2 knock-in allele

In order to test the functionality of the IREShP1/mP2 knock-in allele western blot analysis was performed on mouse tissues before and after the deletion of the NEO resistance cassette. Deletion of the NEO cassette was achieved by crossing the IRES-hP1/mP2 mice with a FLP deleter strain (IRES-hP1/P2 ΔNEO). Subsequently IRES-hP1/P2 ΔNEO mice were crossed with Cre deleter mice in order to excise the human profilin1 (hP1) gene and induce mouse profilin2 (mP2) expression (IRES-P2 ΔNEOΔhP1). Since thymus and spleen have high expression levels of profilin1 (P1) and since mP2 should be transcribed under the control of profilin1 promoter, those tissues were tested for the expression of P2 in mice heterozygous for the knock-in allele (Figure 5).

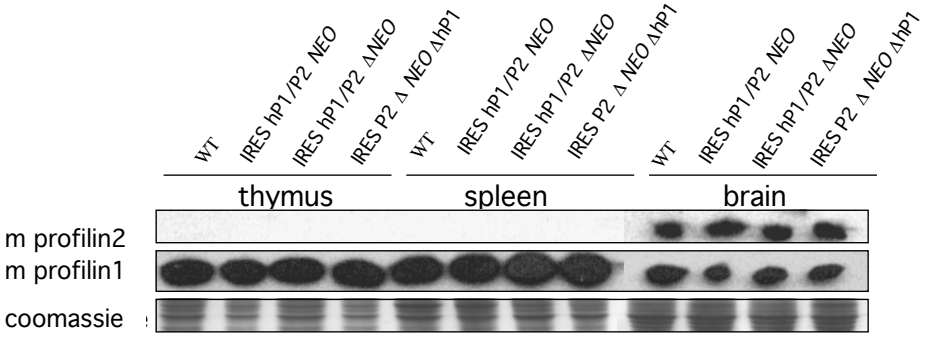

Figure 5 Western blot analysis of protein extracts from thymus, spleen and brain of IRES-hP1/mP2 knock-in mice.
No profilin2 was detected in thymus and spleen extracts after replacement of the endogenous profilin1 by the IRES-hP1/mP2 cassette using the 3003 antibody. Endogenous expression of profilin2 in the brain of these mice was not altered. Profilin1 expression detected with P1-T antibody shows the expected pattern, before and after each deletion. Equal loading was confirmed by coomassie staining.

No profilin2 expression was detected in spleen and thymus of heterozygous IRES-hP1/mP2 knock-in mice. Endogenous profilin2 expression was not altered in the brain of knock-in mice. Profilin1 expression level from the WT allele was not altered in these mice.

2.1.4 Alternative replacement strategy by direct knock-in of the profilin2 cDNA into the profilin1 locus

Since IRES sequences do not always work reliably (Paulous et al. 2003) this might be an explanation for the absence of profilin2 expression. Therefore, I decided to use a second approach, where the coding sequence for profilin2 is fused directly to the ATG of profilin1 (4.1.2). In this construct the profilin1 promoter structure is maintained and the profilin1 translation start site is used. The NEO resistance cassette can be conditionally removed by FLP recombination (Figure 6A). The targeting vector was electroporated into ES cells and 196 clones were picked and expanded (4.2.1a).

A

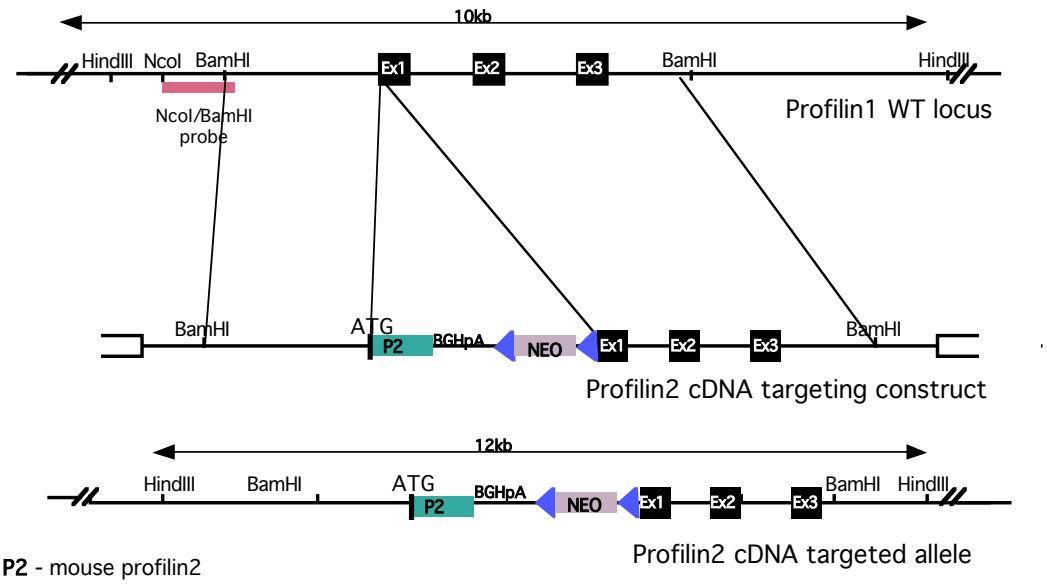

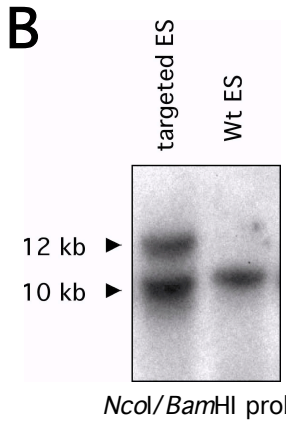

Figure 6 Targeting strategy of the profilin2 cDNA into profilin1 locus.

A) Schematic drawing representing the profilin1 wild type region, the targeting construct and the targeted allele where profilin1 is substituted by the profilin2 cDNA fused to the start codon of profilin1.

B) Southern blot analysis of genomic DNA from homologous recombinant ES cell and wild type clones digested with *Hind*III. After probing with *Ncol/Bam*HI external probe the right pattern confirming homologous recombination event was identified.

After *Hind*III digestion of ES cell genomic DNA and Southern blot analysis with the external *Ncol/Bam*HI probe, two bands were identified, one of 10 kb, belonging to the WT allele and one of 12 kb belonging to the targeted allele (Figure 6B). The shift in size results from the insertion of the profilin2 cDNA and neomycin resistance cassette (Figure 6A). Five ES cell clones were correctly targeted. Single copy integration into the profilin1 locus was confirmed by probing with a NEO probe (data not shown).

2.1.5 Generation of profilin2 cDNA knock-in mice

Two correctly targeted ES cell clones (#3 and #7) were injected into C57 blastocysts. Eighteen male chimeras were generated and mated with wild type C57 females for germline transmission. Agouti offspring were genotyped by PCR using a specific pair of primers amplifying a fragment of the neomycin resistance cassette. The design of the targeting construct outlined in Figure 6A enables the conditional removal of the NEO cassette upon FLP recombination (P2cDNAΔNEO). The same PCR strategy that was used for the screening of IRES-hP1/P2ΔNEO mice was applied to genotype the P2cDNAΔNEO mice (primers #5 and #6 in Figure 4).

2.1.6 Profilin2 expression from the profilin2 cDNA knock-in allele

Western blot analysis was performed on the tissues isolated from the profilin2 cDNA knock-in mice before and after deletion of the NEO resistance cassette. Profilin2 expression in thymus and spleen of the profilin2 cDNA knock-in mice was udetectectable, suggesting that also the P2 cDNA knock-in approach was not successful (Figure 7).

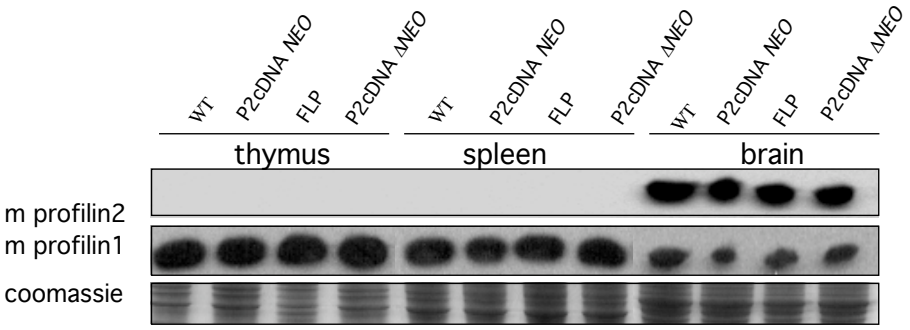

Figure 7 Western blot analysis of the protein extracts isolated from thymus, spleen and brain of profilin2 cDNA knock-in heterozygous mice.
3003 polyclonal antibody recognizing the C terminus of mouse profilin2 did not detect profilin2 expression in thymus and spleen isolated from profilin2 cDNA knock-in mice, regardless of the deletion of the NEO cassette. Probing with P1-T antibody shows that profilin1 expression is not changed in these mice. Presence of the Flp transgene did not interfere with profilin expression. Coomassie staining shows equal sample loading.

2.1.7 Studies on functional redundancy between profilin1 and 2 in mice, conclusions

The approaches used to substitute profilin1 by profilin2 *in vivo* the IRES-hP1/mP2-NEO and the P2cDNA knock-in strategies did not result in detectable expression of profilin2 from the mutated alleles.

2.2 Role of the profilins ligand Mena in neuronal cell development, brain physiology and behavior

Mice where profilin1 expression is reduced to 50% in the Mena null background die in the course of embryogenesis due to the defects in cell migration related to neuronal tube closure. Mena expression is localized in brain, fat, ovaries and testes. As profilin2 is brain specific, I was interested in studying the interaction between Mena and Profilin2 *in vivo*. I decided to compare the profilin2 and Mena KO mouse models with respect to neuronal cell and behavioral phenotype in order to bring new elements to demonstrate the hypothesis that the two proteins act on a common pathway. The behavioral analysis performed on profilin2 KO mice by Alessia di Nardo and Pietro Pilo Boyl in our laboratory showed hyperactivity, altered response to stress and age-dependent impairment in balance and coordination. *In vitro* cultured hippocampal neurons, isolated from Profilin2 KO mice, showed that the lack of profilin2 stimulates neurite outgrowth. In the following chapters I will focus on the effects of the Mena mutation in neuronal cells development and physiology and its further implications for mouse behavior.

2.2.1 Morphology and cytoskeletal organization of Mena KO hippocampal neurons

A number of morphological changes, which occur during the establishment of neuronal polarity, are dependent on actin cytoskeleton dynamics. Growth cone movement to its synaptic target is powered by dynamic rearrangements of the actin cytoskeleton. Filopodial spikes punctuate to the growth cone periphery. The intervening space between filopodia contains a lammelipodium-like branched actin filament network. Actin polymerization in the growth cone drives membrane protrusion. The Ena/VASP protein family is involved in the overall cell motility by

regulating of the actin filament length at the growth cone periphery (Bear et al. 2002). Mena is concentrated at filopodial tips in the growth cone (Lanier et al. 1999), where it may regulate filopodial extension and stability in a manner analogous to that proposed for melanoma cell filopodia (Svitkina et al. 2003). According to these observations, neurons deficient for the Mena gene might exhibit alterations in the response to the guidance cues, related to changes in the integrity of growth cone formation and function.

In order to elucidate the role of Mena in neuronal cells a comparative analysis between wild type (WT) and Mena KO (KO) hippocampal neurons was performed. Intercrosses between heterozygous mice for the Mena mutation were set up and at day E16.5 embryos were dissected and genotyped, and hippocampal neurons were prepared as described (4.2.2a). At this stage hippocampal neurons are undifferentiated. Shortly after plating, cells attach to the extracellular matrix and pass through specific morphological changes in a defined sequence that eventually leads to neuronal polarization. Initially neurons are unpolarized (stage1). After 6-12 hours in culture short neurites appear, followed by the outgrowth of minor processes that do not show differences in morphology (stage2). Within 48 hours in culture one of the processes elongates more extensively than others: the establishment of the axon defines cell polarization (stage3). After 12 - 16 days in culture hippocampal neurons are able to form functional synapses as they have gained all the features of mature neurons (Craig and Banker 1994). In my studies, I determined neurite length and cell body area to compare neuronal differentiation in the wild type and Mena deficient hippocampal neurons. Neurons were followed by light microscopy at four different time points after plating: 6, 24, 48 and 72 hours (4.2.2b) Phase contrast pictures were captured and data regarding neurite length and cell body area were collected in seven separate neuronal preparations and analyzed with Image J 1.29X (NIH, Baltimore, USA) and Stat View 5.0 (Abacus Concept, Berkley, USA) for statistical analysis. Figure 8A contains representative images of neurons. The majority of the hippocampal neurons deficient for Mena

produced primary processes already within 6 hours after plating while neurons isolated from WT mice merely settled. 6h, 24h and 48h after plating the length of the primary processes in Mena KO neurons were significantly longer than those in WT cells (6h, +150%, P<0.001; 24h, +32%, P<0.05, 48h, +37%, P<0.01, one-way ANOVA, Figure 8B). However 72h after plating the length of the dendritic processes between Mena KO and WT neurons were similar. Measurement of the cell body area revealed that Mena KO neurons 6h and 24h after plating are spread significantly more compared to WT cells (6h, +60%, P<0.001; 24h, +30%, P<0.001, one-way ANOVA, Figure 8C). 48h after plating measurements of the cell body area of WT and Mena KO neurons appeared to be equal. Cell body area of Mena KO neurons seems to reach a plateau in size around 24h *in vitro* while WT cells keep spreading for another 24h.

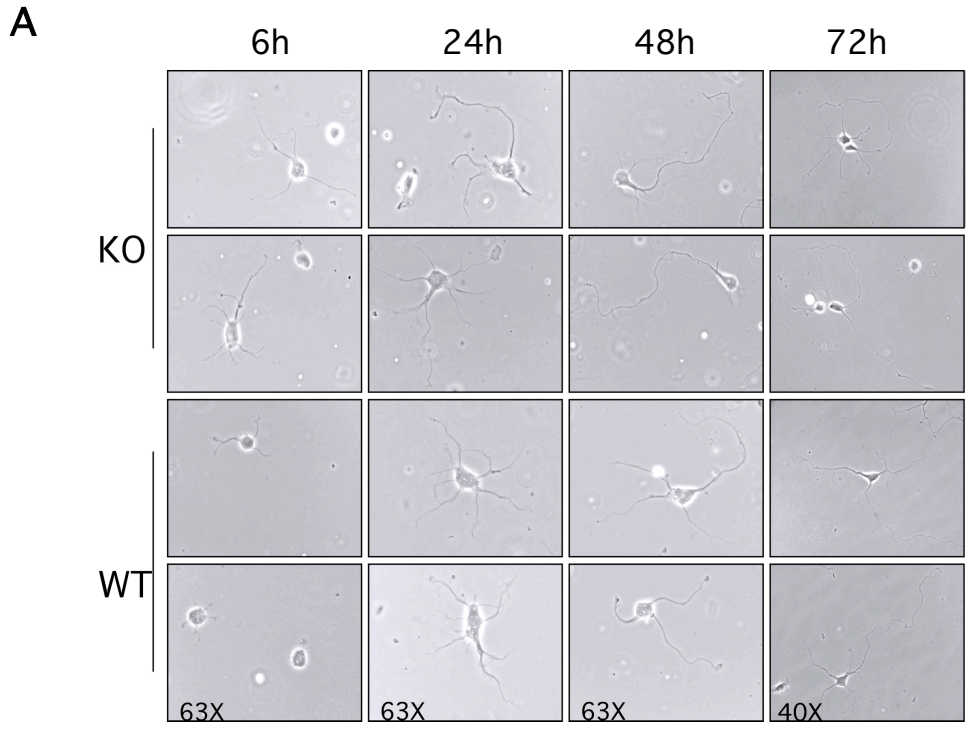

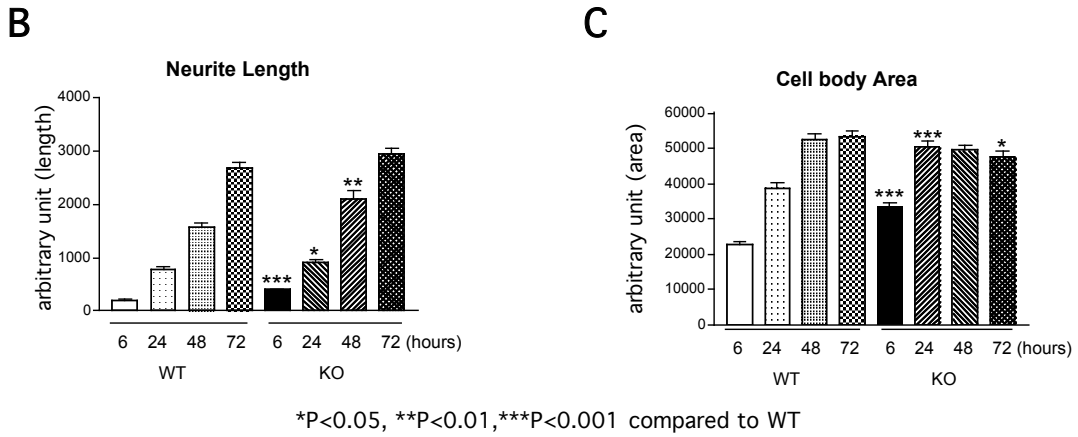

Figure 8 Morphological analysis of E16.5 cultured hippocampal neurons.
A) Representative images (light microscopy) of the hippocampal neurons isolated from WT and Mena KO mice 6h, 24h, 48h and 72h after plating.
B) Neurite length of Mena KO neurons 6h, 24, 48h after plating is significantly longer compared to the WT cells ($P<0.001$;$P<0.05$; $P<0.01$, one-way ANOVA). At the latest time point examined (72h) neurite length is comparable between WT and Mena KO neurons.
C) Cell body area of the Mena KO neurons 6h and 24h after plating is significantly larger compared to the WT cells ($P<0.001$, one-way ANOVA). At 48h and 72h time points cell body area is comparable between WT and Mena KO neurons.

2.2.2 Mena does not play a role in glutamate and NMDA mediated neurodegeneration

A growing body of evidence suggests that in addition to the regulation of the cell structure and motility, actin filaments may be involved in the modulation of ion channels function (Johnson and Byerly 1993; Rosenmund and Westbrook 1993; Berdiev et al. 1996). Several actin-binding proteins like gelsolin, spinophilin and PSD-Zip45 (Homer 1c) have been implicated in coupling actin cytoskeleton dynamics with neurotransmission (Furukawa et al. 1997; Smith et al. 1999; Usui et al. 2003). Gelsolin for example is involved in the opening and closure of NMDA receptors and voltage dependent calcium channels (Furukawa et al. 1997). Therefore I was interested in whether Mena might play a role in ion channels regulation through modulation of the actin cytoskeleton.

In a first approach I decided to investigate the sensitivity of Mena-deficient cortical neurons to glutamate and NMDA insults (4.2.2g). Cortical neuronal cultures from E16.5 embryos were established as described (Schubert and Kaprielian 2001). On day eight of culture, WT and Mena KO neurons were subjected to a 10 min insult of glutamate or NMDA. Cell viability was evaluated after three days from the insult via MTS assay (4.2.2h). Cell survival mean values were calculated from the treatment of five distinct neuronal cultures. One-way ANOVA analysis did not show any genotype effect neither for glutamate nor for NMDA excitotoxicity (P= 0.079, one-way ANOVA Figure 9A,B,C).

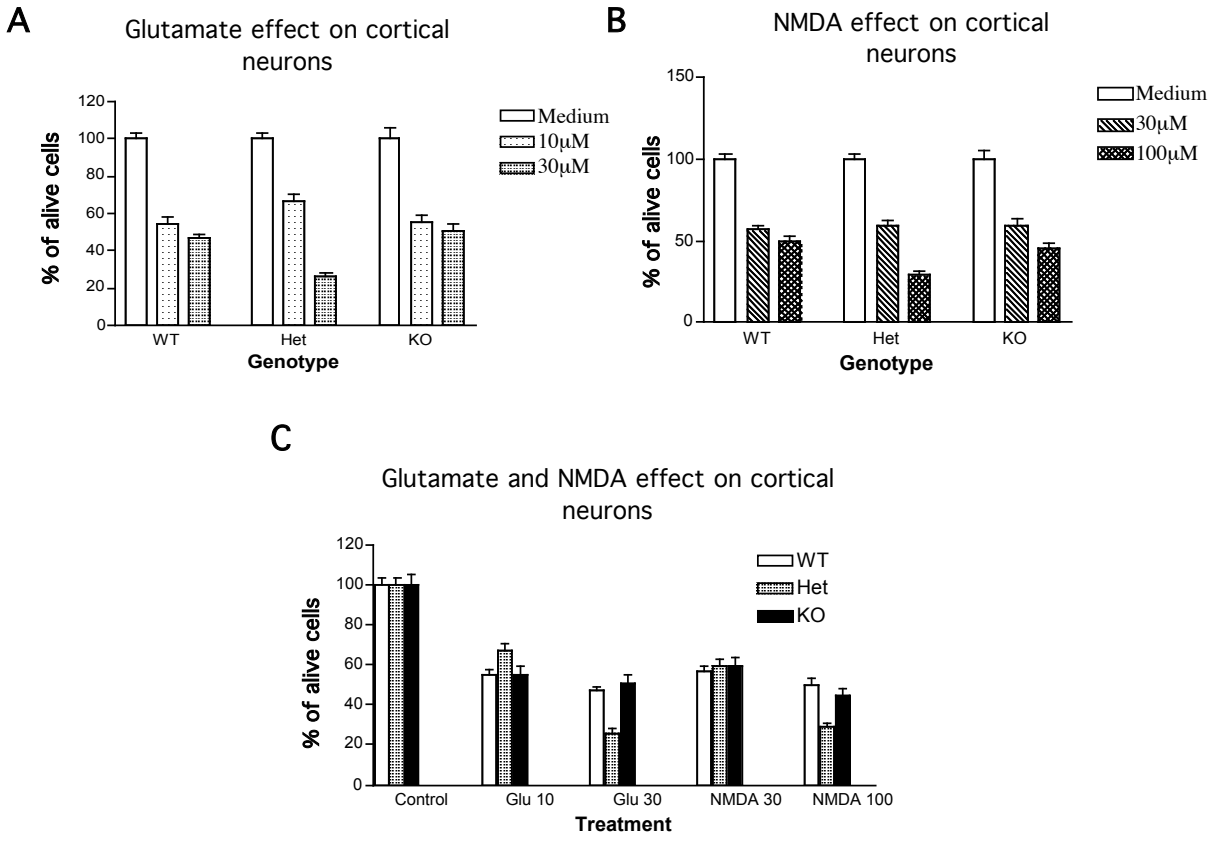

Figure 9 Glutamate and NMDA effect on cortical neurons.
A) Increasing concentrations of glutamate resulted in an increased level of apoptotic cell death in all genotypes: wild type (WT), heterozygous (Het) and homozygous for Mena mutation (KO) **B)** The same tendency as in A) was observed upon NMDA insults. **C)** Summary of glutamate and NMDA treatments on cortical neurons. The excitotoxic effect of glutamate and NMDA on cortical neurons is independent from the Mena mutation.

2.2.3 Mena KO neurons have an increased sensitivity to Menadione induced oxidative stress

My initial findings that Mena plays no role in the neurodegeneration processes regulated by NMDA/glutamate receptors, led me to the question whether this adhesion/actin binding protein might be important in the cellular response related to non–receptor controlled cell death upon oxidative stress. In order to address this issue WT and Mena KO cortical neurons, prepared as described (4.2.2a), were maintained in culture for 48 hours exposed to Menadione and analyzed via MTS assay (4.2.2h). Menadione is a quinone that is metabolized by the proapoptotic flavoprotein reductase to semiquinone, which can be oxidized back to quinone in the presence of molecular oxygen. This cycle is associated with the increased production of reactive oxygen species that are known for their high cellular toxicity (Ko et al. 2000). Cytoskeletal components constitute one of the principal targets of Menadione induced oxidative damage through ATP depletion, partial mitochondrial depolarization, cytochrome C release, thiol depletion, Tau dephosphorylation and elevation of the total cytosolic Ca^{2+} concentration (Thor et al. 1982; Di Monte et al. 1984; Nicotera and Orrenius 1992).

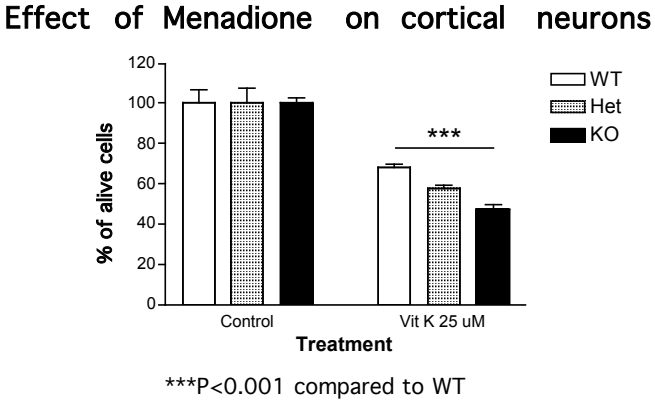

Figure 10 The oxidative stress effect on cortical neurons upon Menadione treatment.
Mena-deficient (KO) cortical neurons are more sensitive to the drug insult with respect to wild type (WT) (-36%, P<0.001, Bonferroni/Dunn t test) and heterozygous (Het) cells (-18%, P=0.001, Bonferroni/Dunn t test). Increase in the response of these neurons to oxidative stress is gene dosage dependent.

Mena KO cortical neurons showed significantly enhanced vulnerability to the drug when compared to the wild type (-36%, P<0.001, Bonferroni/Dunn t test) and heterozygous cells (-18%, P=0.001, Bonferroni/Dunn t test). Already 50% reduction of Mena leads to the sensitization of the cortical neurons to Menadione insult, suggesting that this effect is gene dosage dependent.

2.2.4 Consequences of the Mena mutation on behavior

Communication between telecephalic hemispheres occurs through three major commissures: the corpus callosum (CC), the hippocampal commissure (HC) and anterior commissure (AC) (Abbie, 1940). In Mena KO mice axons that are projecting from inter hemispheric cortico-cortical neurons are misrouted in early neonates and fail decussation from the corpus callosum. Defects in the hippocampal commissure and ponto-cerebellar pathways were also observed in these mice, suggesting an important role of Mena in axon path-finding. To date no studies have been performed addressing the question whether the axon path-finding defects result in physiological alterations that can affect the behavior of the Mena KO mice. Therefore I decided to analyze the behavior of Mena KO mice and compare it to the findings from the profilin2 KO mice. All the behavioral tests were performed in the collaboration with the Phenotyping Core Facility (Dr Anne Cécile Trillat Group), EMBL-Monterotondo

2.2.5 Animals

Mena mice were generated as described (4.4.1) on a mixed genetic background. To obtain congenic Mena mutant mice, Mena heterozygous animals (Mena Het) were mated with wild type C57BL/6 (The Jackson Laboratory, Bar

Harbour, ME) for 10 generations. Heterozygous mice were then intercrossed to generate animals in which both copies of Mena were deleted.

2.2.6 Breeding strategy and Mena KO mice survival

At the age of three weeks pups born from heterozygous breeding pairs were genotyped. Our results showed significant loss (-50%) of Mena KO mice within the first three weeks. Examination of mice revealed that the Mena KO young mice, mainly males, were often smaller in size and appeared dehydrated compared to control littermates.

Genotype / number	WT	Het	KO
Expected	31.25	62.5	31.25
Obtained	36	75	14

Table 2 Results of the breeding between mice heterozygous for Mena mutation.
50 % less of the Mena KO mice were weaned with respect to the expected 25% ratio.

2.2.7 Time line of behavioral tests

A group of thirty-one animals composed of wild type, heterozygous and homozygous Mena mutant mice of different age and gender (Table 3) was subjected to the panel of behavioral tasks summarized in Figure 12. Mice were single housed for one week before the tests and remained in such housing conditions until the end of the experimental series.

	Males		Females	total
	3-4 month old	10-16 month old	3-4 month old	
WT	3	4	3	10
Het	3	3	4	10
KO	3	4	4	11

Table 3 Composition of the population of Mena mutant mice subjected to the primary behavioral phenotyping panel.

To make optimal use of the available animals, we performed the following sequence of behavioral tasks with the same animals. Animals were tested and allowed to rest as described in Figure 11.

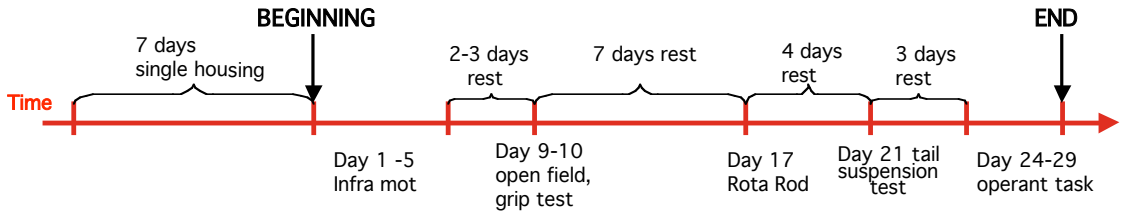

Figure 11 Schematic drawing of the behavioral task panel calendar used to assess Mena mice primary behavioral phenotype. Resting periods are indicated.

The behavioral task panel was designed to assess basic behavior of Mena KO mice. Figure 12 groups the assays by type of functions addressed.

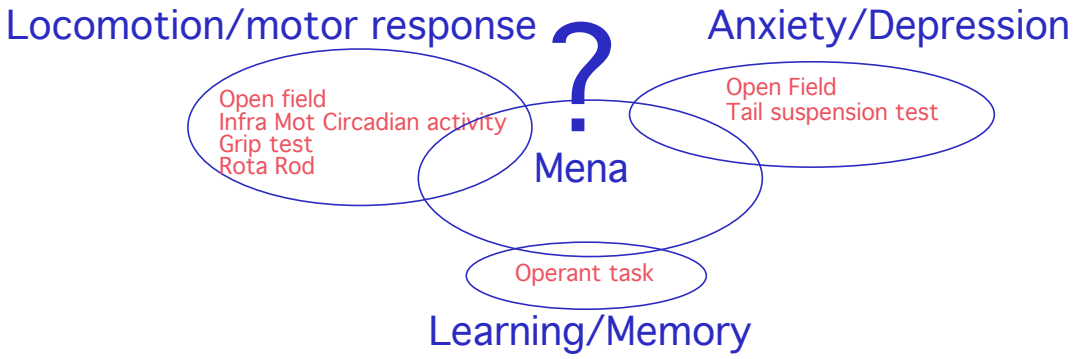

Figure 12 Schematic drawing of the behavioral task panel used to investigate the effect of the Mena mutation in mice. Tests are grouped according to the functions they address.

2.2.8 Body weight

We observed that at weaning age some pups in the litter were much smaller than the rest, therefore we decided to follow up the body weight of these mice. In order to address this issue the body weight of 31 mice (Table 3) was measured before starting the behavioral task sequence. Our results show that mice carrying the Mena mutation suffer from significant reduction in body weight (-22%, $P<0.05$ when compared to the WT group, one-way ANOVA, Figure 13A).

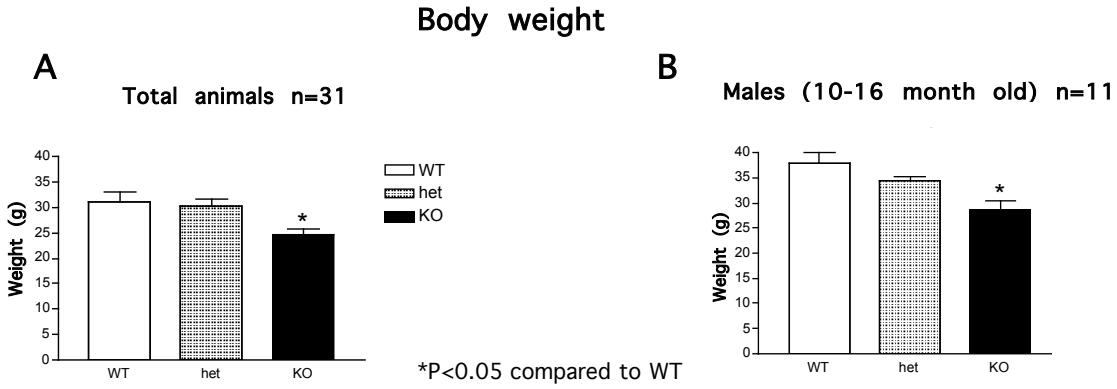

Figure 13 Body weight measurement
A) Mena-deficient mice (KO) show a significant reduction in body weight when compared to wild type animals (WT) (-22%, $P<0.05$, one-way ANOVA).
B) Reduction in the body weight increases with the age of Mena KO mice (-28%, $P<0.05$, one-way ANOVA).

Further analysis suggests that the decrease in body weight is even more pronounced in aging males (-28%, P<0.05 when compared to the WT group, one-way ANOVA, Figure 13B). In order to explain the origin of body weight deficiency in Mena KO mice we dissected and weighted front leg muscles and fat pads. No difference was observed in Mena-deficient mice regarding muscle weight compared to the wild type group (Figure 14 A, B).

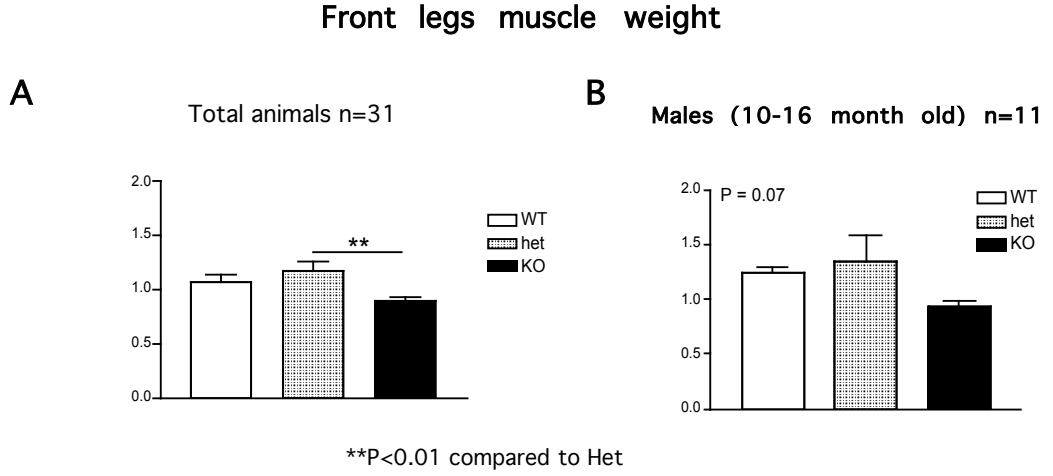

Figure 14 Front legs muscle weight measurement.
A, B) There is no difference in front legs muscle weight between wild type and Mena KO mice, regardless of animal age.

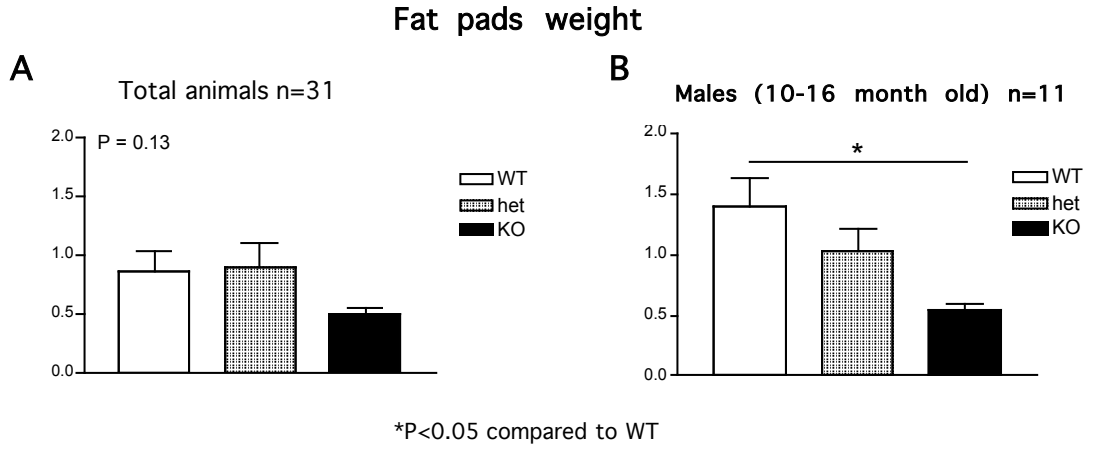

Figure 15 Fat pads weight measurement.
A) Mena KO mice show a tendency to have a reduced fat pad weight. **B)** The reduction in fat pads weigh is significant in aging KO mice (-68%, P<0.05, one-way ANOVA).

Measurement of the fat pad weight revealed a deficit in Mena KO mice (P=0.13, Figure 15A). Again, the difference becomes more significant in aging males (-68%, P<0.05 compared to WT mice, one-way ANOVA, Figure15B).

2.2.9 Home cage activity and circadian rhythm are not altered in Mena KO mice

The significant reduction in both body weight and survival observed in Mena KO mice suggested a potential impairment of the basic activity of these mice. In order to address this issue, total locomotor activity during the light and the dark phase for five consecutive days was measured using the Infra Mot test system (4.5.1).

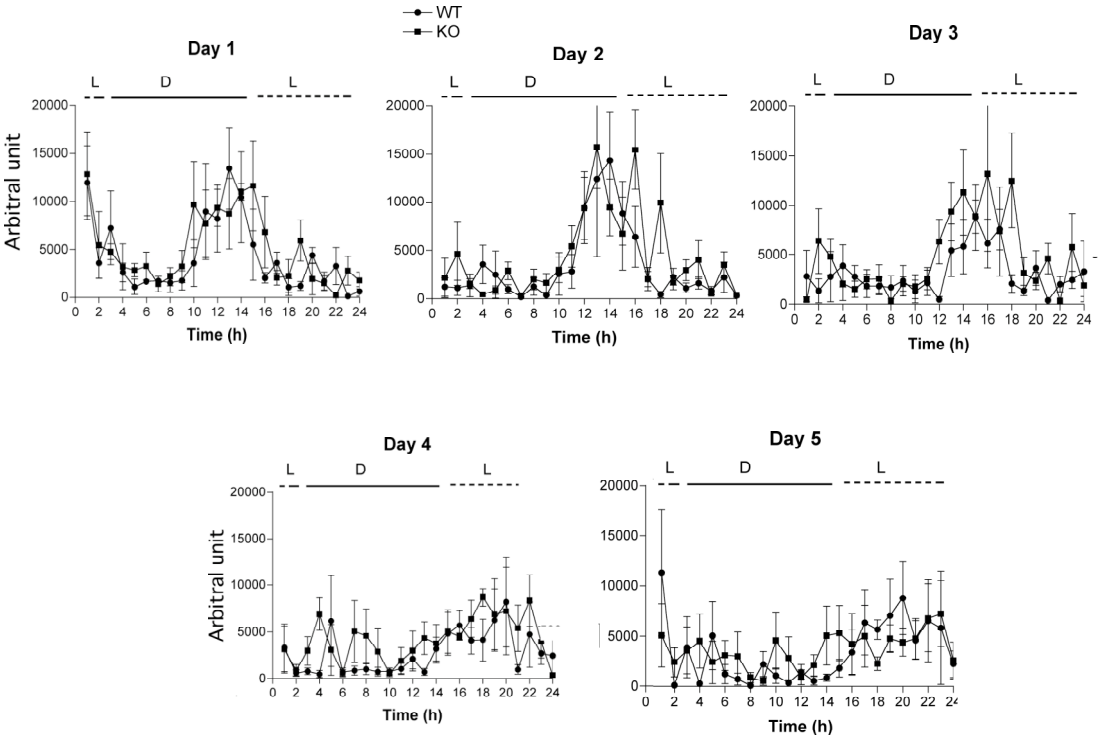

Figure 16 Locomotor and circadian activity of wild type (WT) and Mena KO (KO) mice over a 24h time period for 5 consecutive days. A subset of 8 male mice (n=4 for WT and n=4 for Mena KO, 3-4 month old) was tested. There was no significant difference between the two groups at any day of the test (two-way ANOVA).

Neither a genotype effect, nor an interaction between the genotype and time was observed, suggesting that the general locomotor activity is similar in Mena KO and wild type mice (Figure 16).

2.2.10 Mena KO mice display decreased locomotor activity in an open field test

The animal body shows a high level of integration: muscles are innervated by motor neurons, spinal and cranial motor neurons are innervated by hind brain neurons in the medulla and cerebellum, hindbrain neurons are innervated by projections from the midbrain and forebrain and the motor cortex contributes the highest level of governing. Mena mutants show anatomical changes in the corpus callosum and the hippocampal commissure, and axons are misrouted in Mena KO neonates (Lanier et al., 1999). This axon path-finding defect may result in the impairment of motor function of the Mena KO mice.

In order to study locomotor activity, I placed the animals (Table 3) in the open field and tracked their path for 60 min (4.5.2). The path length (mm) was measured every 5 min in both the center and at the periphery of the open field. The data were analyzed using two-way ANOVA for repeated measures. No difference in locomotor activity was found between WT and KO mice when the animals were grouped according to the genotype (Figure 17A). However the analysis of the 10 -16 month old male mice revealed that Mena KO mice display a lower locomotor activity when compared to wild type mice (genotype effect P=0.0179, two–way ANOVA for repeated measures, Figure 17B). It is interesting to note that both WT and KO mice seem to habituate to the open field similarly (no genotype/time interaction effect) (Figure 17C).

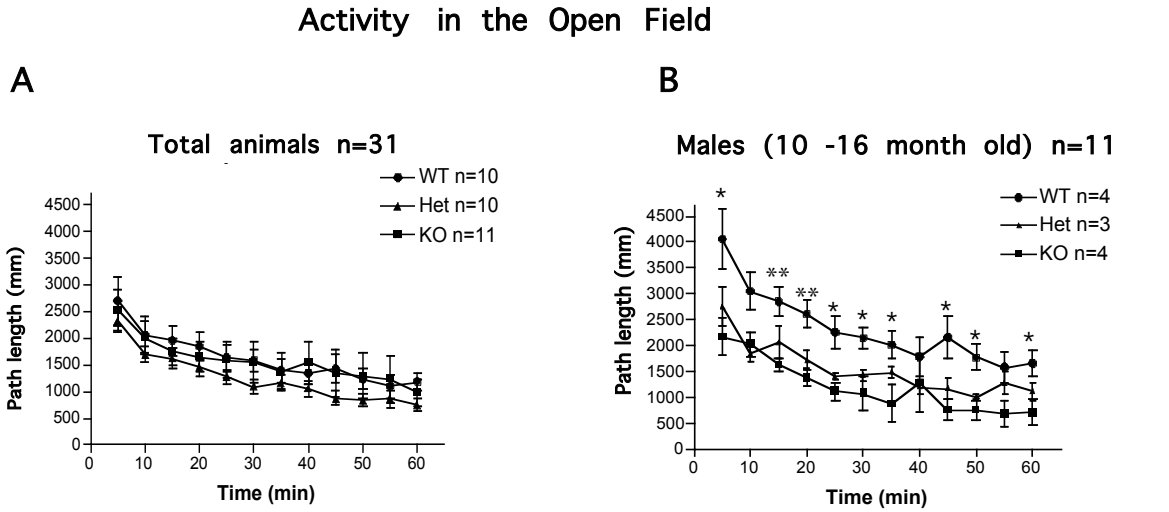

*P<0.05, **P<0.01 compared to WT

Open field

Factor	All n=31	Males n=20	Females n=11	Males (10-16 month old) n=11
genotype	0.56	0.10	0.40	0.0179
time	<0.001	<0.001	<0.001	<0.001
interaction	0.96	0.95	0.12	0.41

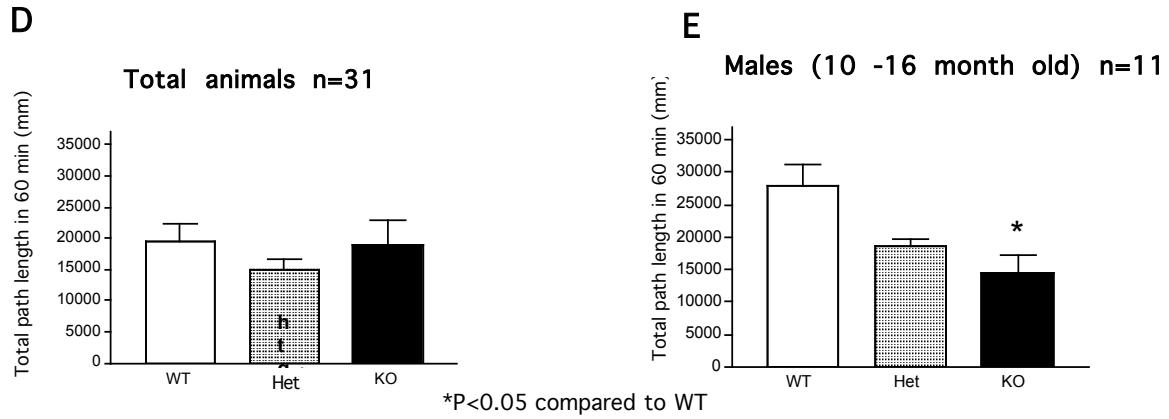

*P<0.05 compared to WT

Figure 17 Locomotor activity (mm) in a 60 min open field.
A) Measurements of the distance traveled in the open field every 5 min by a total of 31 animals grouped by genotype. No difference in locomotor activity was observed between wild type (WT) and Mena KO (KO) mice (P=0.56) **B)** The group of 10-18 month old Mena KO mice show less locomotor activity that WTs (P=0.0179, two-way ANOVA). **C)** P values calculated for the genotype, time and interaction effects by two-way ANOVA in the 60 min open field test. **D)** Total path measurement confirmed no difference in locomotor activity when mice are grouped by genotype only. **E)** Significant reduction in the total path length was shown by Mena KO aging males (47%, P<0.05, two-way ANOVA).

I also calculated the total path length during the entire 60 min session (one - way ANOVA). The analysis of the total path length over 60 min confirmed the previous findings when the animals were grouped according to the genotype (Figure 17D), and revealed that 10 -16 month old Mena KO males exhibit an impaired locomotion (47% reduction, P<0.05 compared to WT, one–way ANOVA, Figure 17E).

2.2.11 Motor coordination, balance and motor learning in Mena KO mice

The expression pattern of Mena in the cerebellum, particularly in the Purkinje cells, suggests a potential role of Mena in motor coordination and balance. In order to test this hypothesis, a group of 30 mice (WT n=9, HET n=10, KO n= 11) was subjected to the Rota Rod test as described (4.5.3). I measured both the latency to fall off the rod and the speed at which the animals fell. I found that Mena KO mice show significant reduction in the latency to fall when compared to WT mice, Figure 18A (genotype effect P=0.03, two-way ANOVA for repeated measures on latency).

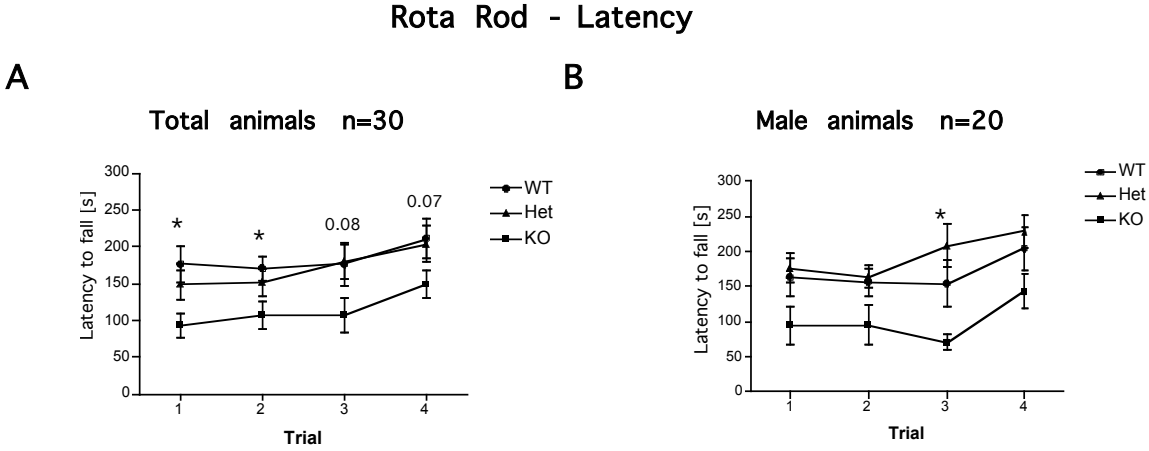

*P<0.05 compared to WT

C

Rota Rod latency

Factor	All n=30	Males n=19	Females n=11	Males (10-16 month old) n=10
genotype	0.03	0.02	0.25	0.07
trial	<0.001	<0.007	0.04	0.02
interaction	0.86	0.50	0.83	0.87

Rota Rod - RPM

D

Total animals n=30

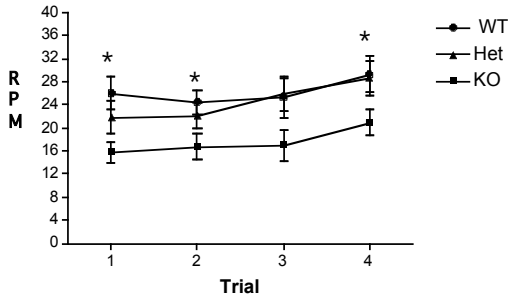

E

Males (10 -16 month old) n=10

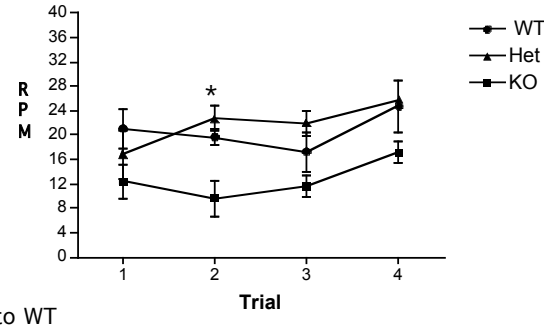

*P<0.05 compared to WT

F

Rota Rod RPM

Factor	All n=30	Males n=19	Females n=11	Males (10-16 month old) n=10
genotype	0.02	0.09	0.09	0.04
trial	<0.001	0.003	0.09	0.05
interaction	0.79	0.76	0.82	0.7

Figure 18 Rota Rod – motor coordination and motor learning
A) Average latency to fall off the rod measured in four separate trials was significantly shorter for Mena KO animals compared to WTs. **B)** The impaired performance was seen in Mena KO males regardless of their age. **C)** P values regarding genotype, trial and interaction effects by two-way ANOVA for repeated measures on latency to fall. **D)** Measurements of the speed at which animals were falling off the rod confirmed impaired performance in Mena KO mice. **E)** The genotype effect results from aging Mena KO males. Nevertheless both WT and Mena KO animals showed an improvement in motor learning upon training. **F)** P values regarding genotype, trial and interaction effect by two-way ANOVA for repeated measures on RPM.

Detailed analysis of the latency to fall among the animals in the group revealed that the low performance of males was responsible for this result Figure 18B (genotype effect P=0.2, two-way ANOVA for repeated measures on latency). In addition Mena KO mice fell at a lower speed than WT mice, Figure 18D (genotype effect P=0.02, two-way ANOVA for repeated measures on RPM). Again, this effect can be explained by the poor performance of 10 -16 month old Mena KO males (Figure 18E). In addition I found the same significant trial effect for the two genotypes, measuring both the latency to fall off the rod and speed at which animals fell, indicating that WT and Mena KO mice have similar motor learning skills (Figure 18C,F).

2.2.12 Grip test – muscle strength

Impaired performance of the Mena KO mice in the Rota Rod test might implicate a function of Mena in motor neuron innervation of the muscle. In order to address the question whether the decreased locomotor activity observed in Mena KO mice is caused by impairment in muscle function, I performed the grip test in order to measure muscle strength (4.5.4). A group of 31 mice was subjected to the grip test (Table 3). The muscle strength of front legs and all four legs was measured in three consecutive trials. The mean of the three trials was calculated. Mena KO mice showed a tendency to be weaker when compared to WT animals (P=0.055 Figure 19A). The same tendency was observed in aging Mena KO males (Figure 19B).

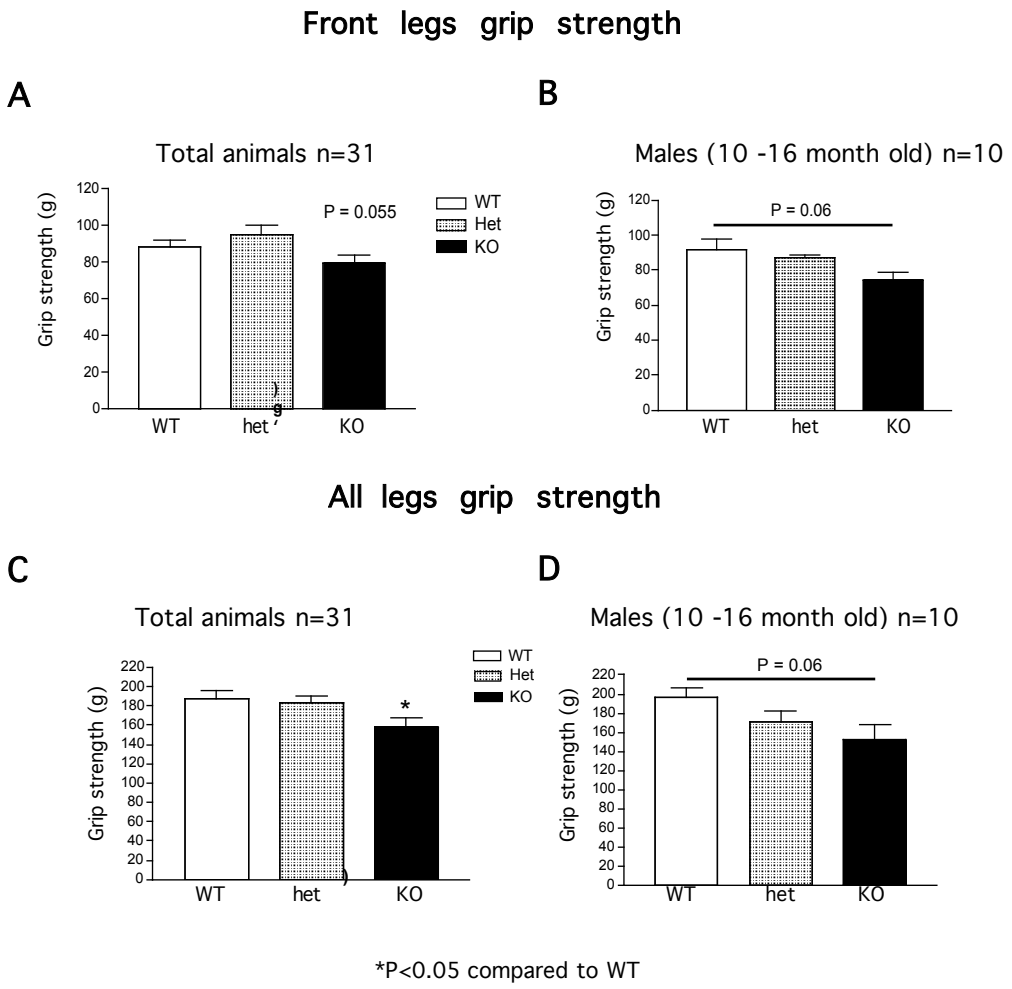

Figure 19 Grip test - muscle strength.
A) Mena KO mice show a tendency to have a reduced front legs grip strength. **B)** The same tendency as in A was observed in the group of 10-16 month old Mena KO mice. **C)** There is a significant reduction in the grip strength of all the legs in Mena KO mice (-17%, P<0.05, one-way ANOVA). **D)** The grip strength of all the legs is not significantly reduced in aging Mena KO mice.

When the grip strength of all the legs was considered, I found a significant reduction in the grip strength of Mena KO mice (-17%, P<0.05 when compared to WT mice, one-way ANOVA, Figure 19C). This finding was not confirmed for the aging Mena KO males since the reduction in this case was not significant (P=0.06, Figure 19D)

The reduction in muscle strength of the Mena KO mice observed in the grip test might result from a difference in muscle weight, therefore I normalized the front grip strength by the front legs muscle weight (2.2.8). In this analysis no genotype

effect was found between wild type and Mena KO animals, regardless of their age (Figure 20 A, B). This indicates that Mena KO mice are weaker because they have less muscular mass.

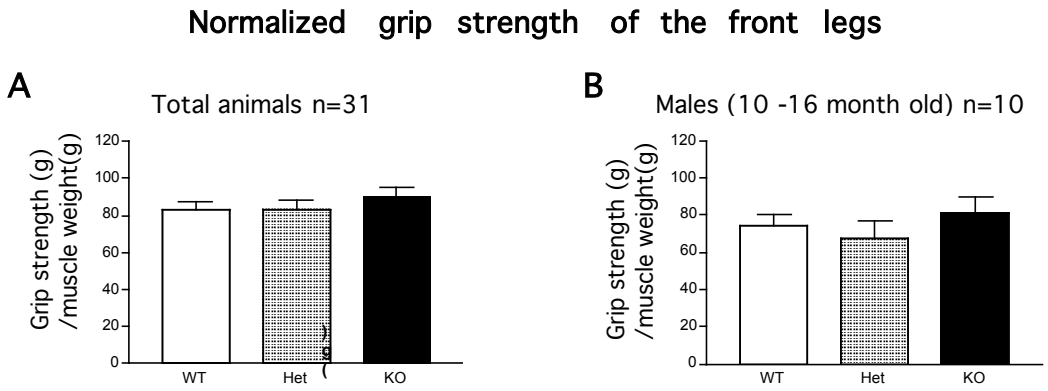

Figure 20 Grip strength of the front legs divided by front legs muscle weight.
A,B) There is no difference in grip strength between WT and Mena KO mice with this analysis regardless of the age of the animals tested.

2.2.13 Tail suspension test

To assess whether depression and stress response are affected by the Mena mutation I performed the tail suspension test. The test consists of a 6 min session where the animal is hung by the tail (4.5.5) and the mobility time is measured. Final results are expressed in immobility time by subtracting the mobility time (animal struggling, curling to get to horizontal position) from the total session time (240 sec). A set of 31 mice (Table 3) was subjected to the test. Mena KO mice showed a significant reduction in the immobility time (70% reduction in immobility time, $P<0.001$, one-way ANOVA, Figure 21A). In a more detailed analysis it appeared that this effect was only observed in males (77% reduction on immobility time, $P<0.001$, one-way ANOVA, Figure 21B) regardless of their age (data not shown) but not in females (Figure 21C).

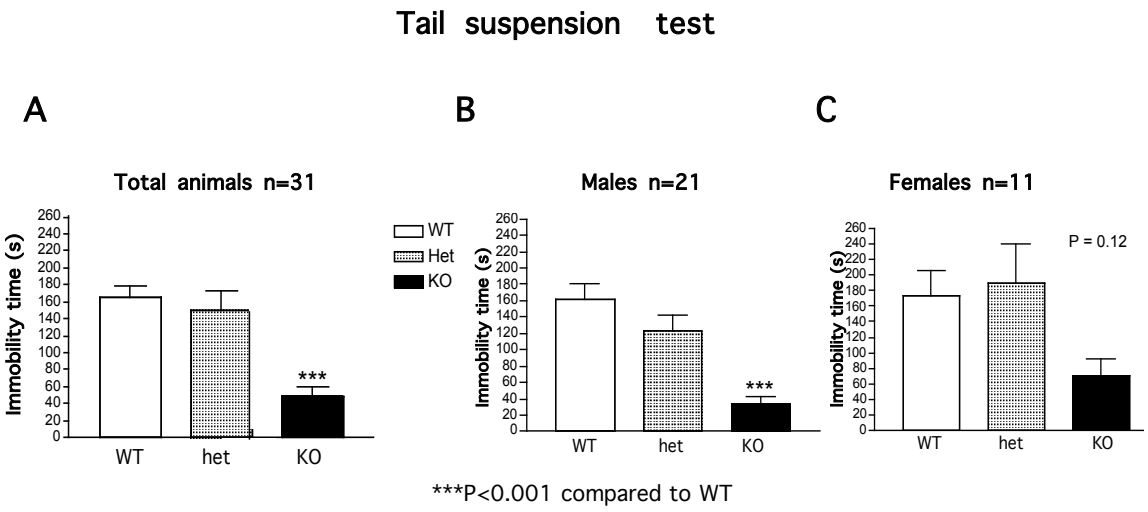

Figure 21 Tail suspension test - depression and stress response.
A) Mena KO mice show significantly reduced immobility time with respect to WT mice (70% reduction, P<0.001,one-way ANOVA). **B)** The observed difference results from the male population of Mena KO animals (77%, P<0.001, one-way ANOVA). **C)** Females deficient for Mena behave similarly to WT females.

2.2.14 Time spent and distance traveled in the center of the open field

Our previous results showed that the total locomotor activity of the Mena KO mice in the open field is reduced (2.2.10). This, together with the observed significant reduction of the immobility time during the tail suspension test (2.2.13), might suggest an altered response to stress resulting, for example, in increased freezing and/or traveling in the periphery of the open field with respect to WT mice.

In order to address this issue I calculated the time spent and the distance traveled by the animals in the center of the open field. The center of the open field is considered to induce stress, therefore mice tend to avoid this area. My results did not reveal any difference in the percent of the path traveled in the center of the open field calculated with respect to the total distance covered by the animals in 60 min session of the test (Figure 22A). In addition, no significant difference in time spent in the center of the open field was observed (Figure 22B).

These results suggest that this type of stress response is not altered in Mena KO mice.

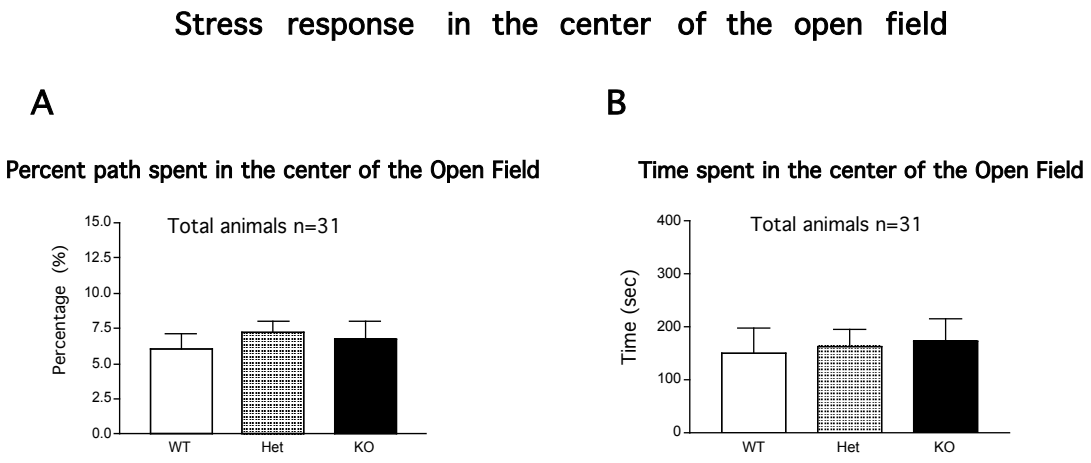

Figure 22 Center of the open field – stress response.
A) Mena KO mice show similar percentage of the path traveled in the center of the open field to WT mice. **B)** No difference was observed regarding time spent in the center of the open field between Mena KO and WT animals.

2.2.15 Operant task - learning and memory

Studies of human commissurotomy indicate that the main interhemispheric communication pathway between hippocampi, the hippocampal commissure, is important for normal memory and learning functions. Since the Mena mutation has been shown to cause alterations in the corpus callosum and hippocampal commissure and in consequence to reduce the hippocampal commissural inputs, I performed the operant task to address learning and memory in the Mena KO mice. A group of 20 males (WT n=7, HET n=6, KO n=7) was subjected to the test as described (4.5.6). No genotype effect was evident looking at the total number of responses between wild type and Mena KO mice (Figure 23A), and no difference between the genotypes was noticed with respect to the number of inoperative responses (Figure 23C). Despite the small size of the group, a tendency to a

reduced number of operative (correct) responses in Mena KO mice was observed (P=0.097, compared to WT, one-way ANOVA, Figure 23B). This might suggest impairment in learning capability of Mena KO mice. In addition I determined the number of the animals that accomplished 50 or more operative responses during the entire session. 6 out of 7 Mena KO mice produced less than 50 operative responses. This further supports my previous observations (Figure 23D).

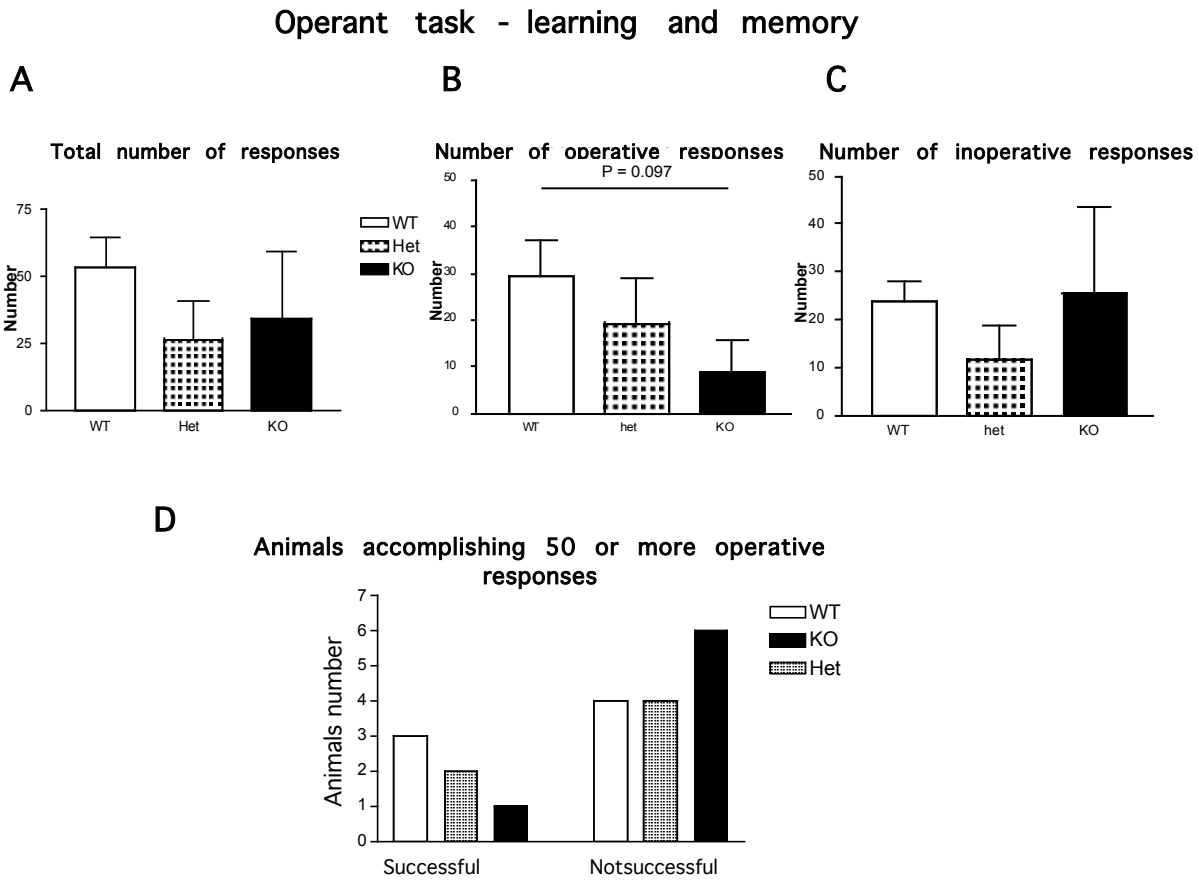

Figure 23 Operant task - learning and memory.
A) The total number of responses (operative and inoperative) measured during the test was comparable between wild type and Mena KO mice. **B)** No difference was observed between WT and Mena KO mice with respect to the total number of inoperative responses. **C)** A tendency to a decreased number of operative responses was observed in Mena KO mice compared to WTs. **D)** Mena KO mice perform poorer when compared to WTs: 6 out of 7 animals did not accomplish 50 correct responses during the entire experimental session.

2.2.16 Phenotype of Mena KO mice - summary

In order to characterize the role of Mena in mice and the possible relation to profilin2 I used cell biology methods and behavioral tools.

My data show that Mena-deficient hippocampal neurons settle and spread faster after plating compared to WT cells. In addition the absence of Mena results in the production of longer primary processes in hippocampal neurons. These findings suggest that Mena may act as a negative regulator of neurite outgrowth.

Cortical Mena KO neurons do not show an increased sensitivity towards glutamate and NMDA excitotoxicity. However, the exposure to Menadione insult shows a higher sensitivity to oxidative stress of Mena-deficient neurons. The anatomical defects lead to alterations in behavior in the Mena mutant mice. Absence of Mena leads to impairment in the locomotor activity, motor coordination, and balance, and the effect of the Mena mutation is always more pronounced in aging animals. Furthermore, lack of Mena appears to alter stress response and impairs learning capability. Summary of our findings regarding Mena behavioral phenotype compared to the wild type is presented in Table 4.

No difference	Tendency	Significant difference
Circadian activity Muscular strength Motor learning	Learning and memory (KO impaired)	Survival (KO impaired) Body weight (KO lighter) Fat pad weight (KO lighter) Locomotor activity (KO impaired, age dependent) Motor coordination and balance (KO impaired, age dependent) Reaction to stress (KO very sensitive)

Table 4 Primary behavioral phenotype of Mena KO mice – summary.

2.2.17 Comparison of Mena and profilin2 phenotypes in mice. Is there a common pathway?

In vitro and *in vivo* studies suggest that Mena and profilin2 interact. The significance of this interaction remains to be elucidated. The comparison of the neuronal cell phenotype and the behavior of mice where either Mena or Profilin2 gene is knocked-out might show similarities that could suggest a common pathway in which the two proteins are involved.

Both Mena and profilin2 KO hippocampal neurons develop faster *in vitro* compared to wild type cells. Hippocampal neurons isolated from Mena KO as well as from profilin2 KO mice (Di Nardo, PhD thesis) settle and spread sooner after plating producing longer primary processes compared to WT neurons.

A comparison of the behavioral phenotypes of Mena and profilin2 KO mice reveals a requirement of both Mena and Profilin2 for coordination and balance. Furthermore both mutations lead to alterations in locomotor activity. However while loss of Mena leads to lower locomotor activity, profilin2 KO mice are significantly hyperactive. The behavioral phenotype of Mena and Profilin2 KO mice is summarized in Table 5.

Activity	Mena KO	Profilin2 KO
Survival	Reduced	Reduced
Locomotor activity	Reduced	Increased
Balance and coordination	Impaired	Impaired
Body weight	Reduced	Reduced
Muscle strength	Reduced	Reduced
Depression and stress response	Altered	Altered as in Mena KO

Table 5 Summary of the Mena and Profilin2 KO primary behavioral phenotypes in comparison to the wild type. Profilin2 KO results were supplied by Di Nardo PhD thesis and Pilo Boyl unpublished data.

3. Discussion

Functional redundancy between profilin1 and profilin2 in mice

The organization of the mouse profilin1 and profilin2 genomic locus is very similar: both isoforms are encoded by three exons spaced by relatively short introns and the exon-intron boundaries are absolutely conserved, suggesting that, given the expression pattern (*Introduction*), profilin2 might have been derived from a duplication of the profilin1 gene. Also biochemically profilin1 and profilin2 are similar with respect to their interactions with the main ligands: actin, PIP_2 and poly-L-proline stretches. However studies on profilin1 and profilin2 in mice showed differences in tissue distribution as well as in ligand binding (Witke et al. 1998; Di Nardo et al. 2000). In addition KO mice for profilin1 and profilin2 display dramatically different phenotypes (Witke et al. 2001; Di Nardo PhD thesis).

Is the profilin-actin interaction the primary function that profilin plays *in vivo?* If yes we might expect functional redundancy between profilin1 and profilin2 in mice.

One way to address this question is to gradually reduce the amount of profilin in cells. Therefore I performed intercrosses between mice heterozygous for both profilin1 and profilin2 mutation aiming at combining the two genotypes. Mice with 50 % reduction of profilin1 in profilin2 null background are fertile, and do not show anatomical alterations. This finding suggests that reduction to half amount of profilin1 and absence of profilin2 are still enough for vital functions. However further investigation in particular on the behavioral phenotype displayed by these mice need to be performed.

In a second approach, to address potential functional redundancy between profilin1 and profilin2 *in vivo* I used two different knock-in strategies trying to

express profilin2 from profilin1 locus. In addition, I believed that in this way the specific function of each of the two proteins might have been elucidated. In the first targeting construct profilin1 was substituted by the IRES-hP1/mP2 cassette (4.1.1). Considering the risk resulting from the replacement of mouse profilin1 by mP2 this strategy enables the conditional knock-in of mP2 upon the removal of hP1. In fact if mP2 is not equivalent to mP1 the phenotype of this mouse would simply be profilin1 KO. Therefore the introduction of hP1 should guarantee the rescue of this phenotype, given that human profilin1 is similar to mouse profilin1 with respect to actin, PIP_2 and poly-L-proline stretches binding and is 98% identitical in amino acid sequence. Moreover the use of hP1 allows an easy and immediate verification of the functionality of the transgene using a specific hP1 antibody. RT-PCR, but not Norther blot, analysis performed on the tissues that display the highest profilin1 expression level showed the presence of the hybrid hP1/mP2 mRNA (data not shown). However, human profilin1 expression from this allele was undetectable and also the removal of the hP1 did not result in profilin2 expression. These results indicate that profilin1 promoter used for transcription control from IRES-hP1/mP2 knock-in allele was functional nevertheless protein translation was either not efficient or abolished. One explanation for the absence of protein expression from the IRES-hP1/mP2 knock-in allele may lie in the use of the IRES, which has in general a lower translation initiation efficiency respect to the standard initiation mechanism from the 5' cap (Paulous et al. 2003). In order to exclude the uncertainty of the IRES translational control, I used a second knock-in approach, where the coding sequence of profilin2 was directly fused to the first exon of profilin1. Unfortunately also this alternative strategy did not result in a detectable expression of profilin2 from the profilin1 locus.

In the light of these results, another reason for the lack of protein expression from both replacing strategies might lie in the design of the targeting constructs. In both cases the coding sequence of mouse profilin2 (mP2) was used for the replacement. It has been shown that the presence of introns as well as

their position can regulate gene expression and might have been important for translatability of the knock-in alleles (Kuge and Richter 1995). Furthermore, the low amount of the hP1/mP2 messenger RNA identified might be also explained by its instability. The use of the BGH 3'UTR and poly(A) signal sequence instead of the endogenous 3'UTR sequence of profilin1 might have altered the stability of the transcript. In order to design a functional knock-in allele, further work will be necessary to test for the function of intronic sequences as well as profilin1 translational control.

Mena as a negative regulator of neurite outgrowth

The second part of my thesis was focused on the role of the profilin ligand Mena in neuronal development and mouse behavior. Mena KO mice exhibit abnormalities in the structure of the corpus callosum and the hippocampal comissure. Such brain alterations may be due to Mena involvement in the modulation of actin dynamics, especially in response to the axonal cues and therefore, to address the effect of the absence of Mena on the cellular level, I analyzed the phenotype of the Mena KO hippocappal neurons.

Comparing the morphology of the WT and Mena KO hippocampal neurons I detected significant differences concerning neurite outgrowth and spreading. Mena deficient neurons appeared to settle and progress quicker after plating when compared to WT cells. Within the first 48 hours from plating the length of the primary processes produced by Mena KO neurons was significantly longer than that of WT neurons. This time period is considered the neuronal polarization time therefore my results suggest that Mena is implicated in the inhibition of polarization. Facing complex environment, growth cones weigh positive and negative cues to make a correct decision. Axon outgrowth appears to be a consequence of rapid remodeling of the cytoskeleton just underneath the cell

surface (Marsh and Letourneau 1984; Bentley and Toroian-Raymond 1986). Attractive cues seem to stimulate local actin assembly (O'Connor and Bentley 1993) whereas repellent cues provoke the collapse of actin structures (Fan and Raper 1995). Mena has been shown to concentrate at filopodial tips in the growth cone (Lanier and Gertler 2000), where it might be involved in the regulation of the filopodial extension and stability. The results presented here support the theory that implicates Mena in the regulation of the cellular response to axon guidance cues. However a direct link between cell surface receptor proteins and the actin based motility machinery still remains to be uncovered.

Within 24h after plating, the majority of Mena KO hippocampal neurons were significantly more spread with respect to WT cells. While the body of Mena KO neurons seemed to reach plateau in size within 24h from plating, WT neurons were still in the process of spreading for another 24h. These results reinforce the hypothesis that Mena is involved in actin cytoskeleton reorganization in response to extracellular cues. Different signaling pathways might link Mena to distinct cytoskeletal changes.

A growing body of evidence implicates tyrosine phosphorylation in the downstream response to axon guidance cues (Van Vactor et al., 1998). Mena has been shown to be phosporylated on a tyrosine residue (Tyr-296) by cAbl kinase (Lanier et al. 1999). Drosophila data suggest that both Ena (*Drosophila* homolog of Mena) and dAbl (*Drosophila* Abl) participate in growth cone motility control linking the signals from the cell surface to the actin cytoskeleton. Moreover attraction or repulsion behavior of the growth cone might be mediated by the phosphorylation state of these proteins (Wills et al. 1999; Bashaw et al. 2000). Another mechanism that might involve Mena in cell adhesion process for the regulation of neurite outgrowth points to the family of Rho small GTPases. Studies on neurons *in vitro* indicate that activation of Rac1 and/or Cdc42 increases axon outgrowth, while activation of RhoA GTPase leads to growth cone collapse or retraction (Luo 2000). My results on the increase in neurite outgrowth triggered

by the absence of Mena might be explained by the potential direct or indirect activation of RhoA through Mena in response to external signal received by the neuronal growth cone. Alternatively Mena might be important in deactivation of Rac1 and /or Cdc42. However both of the above hypotheses require further investigation. A possible approach would be the comparison of the activation state of the small GTPases RhoA, Rac1 and Cdc42 in hippocampal neurons deficient for Mena versus wild type cells.

The above alterations in the morphology of Mena KO hippocampal neurons led to the question whether Mena, as shown for other actin binding proteins, might as well be implicated in ion channels function through actin filaments modulation. Glutamate, despite being the predominant excitatory neurotransmitter in mammalian brain, is also toxic to neurons. The delayed neuronal injury that occurs after intense glutamate stimulation depends on the calcium influx through the NMDA subtype of glutamate receptors. Sustained elevation of the ($[Ca^{2+}]i$) level is potentially toxic and leads to the disruption of cytoskeletal components, including actin filaments (Orrenius et al. 1989), implicating calcium in neurodegeneration disorders from cerebral ischemia to epilepsy and Alzheimer's disease (Mattson and Barger 1993; Wasterlain et al. 1993). Comparative analysis of the response of WT and Mena KO cortical neurons to glutamate and NMDA insults revealed that lack of Mena has no effect on the vulnerability of these cells. This finding suggests that Mena is not involved in the actin cytoskeleton changes leading to neuronal sensitization and apoptosis by the NMDA receptors upon glutamate stimulation as in case of gelsolin (Furukawa et al. 1997).

In the cell, production of the reactive oxygen species may serve as an alternative source of calcium load, which consequently can result in cell death. Menadione insults lead to neurodegeneration through oxidative stress (Laux and Nel 2001). This mechanism does not seem to be controlled by any of the known receptors, therefore it addresses the sensitivity of the intracellular components to superoxide generation and to elevated [($(Ca^{2+})i$] levels, mainly in mitochondria.

Mena KO cortical neurons have shown significantly higher sensitivity to Menadione when compared to WT cells. Moreover significant reduction in cell survival was observed in neurons that are heterozygous for Mena gene disruption, indicating that this effect is gene dosage dependent. The fact that Mena KO cortical neurons showed a dramatic cell death response to Menadione and no response to Glutamate/NMDA insults, suggests that Mena might be involved in the response to oxidative stress, through intracellular machinery possibly influencing actin filament dynamics or kinetics. Involvement of Mena in the control of neuronal cell spreading (2.2.1) might be another link to this speculation.

In mouse Mena is required for coordination, balance and stress response

The alterations in brain structures described in the Mena KO mice (Lanier et al. 1999) were an indication that lack of Mena might result in behavioral abnormalities. I therefore decided to study the primary behavioral phenotype of Mena KO mice.

Intercrosses between mice heterozygous for the Mena mutation revealed a reduction in the number of Mena KO animals expected at weaning. Statistical analysis performed on the embryonic population at day 16.5 of embryonic development resulted in the expected 24% of Mena KO mice while at weaning 50% of Mena KO mice were lost. The Mena KO mice, at this age, mainly males, were often smaller in size and appeared dehydrated. The reduced Mena KO mice survival might be caused by impairments in the basic functions of the organism, like respiration or general motility. In order to address this issue, measurement of the body weight as well as analysis of the general activity of the animals was performed. My results showed that the body weight of Mena KO mice is significantly reduced.

To follow the locomotor activity of mice I used the Infra Mot and the open field tasks. Mena KO mice showed no alterations in the circadian activity in their home cage environment, however the locomotor activity in the novel situation of the open field was significantly reduced. For this effect the age of the animals examined was important. Since placing the animal in the open field is considered as an exposure to stress, lower locomotor activity of Mena KO mice, might result from a non adequate stress response, anxiety and therefore freezing at the wall of the open field. Alternatively it could be physiological or coordination impairment. In order to distinguish these issues, time spent and the distance traveled in the center of the open field was analyzed. Mena KO mice displayed similar resting time in the center of the open field when compared to WT animals, suggesting that lack of Mena is most likely not increasing anxiety. On the other hand to address physiological impairments the Rota Rod and the grip tests were used. Measurements of the latency before the animals fell off the rod as well as the speed at which the fall occurred suggested that Mena KO mice have impaired motor coordination. This result correlates with Mena expression in the cerebellum where its absence might result in alterations of motor coordination, postural control and balance. Once again the age of the animals aggravates the observed phenotype. Age dependent impairments in locomotor activity, motor coordination and balance observed in Mena KO mice might be due to neurodegeneration of the motor neurons. This possibility is consistent with the enhanced sensitivity of the Mena KO neurons to oxidative stress (2.2.3).

In order to distinguish whether the impairment in locomotor activity, motor coordination and balance detected in Mena KO mice results from neurological or muscular defects the grip test was performed. Mena KO mice have shown a tendency to produce less strength with the front legs when compared to WT animals. Taking into consideration that this measure might be affected by the muscle weight, I normalized the grip strength data with the front muscle weight. No difference was detected with normalized values between WT and Mena KO

animals, suggesting that Mena KO mice have reduced muscle mass and therefore tend to be weaker.

The cerebellum is considered as a primary site for motor learning (Schiffmann et al. 1999). Purkinje cells are the only output neurons in the cerebellar cortex. The long - term modifications in synaptic strength of Purkinje cells underlie motor learning (Mauk 1997; Lisberger 1998). Previously discussed possible alterations in actin filament structure of Mena KO neuronal cells, might suggest that synaptic plasticity of Mena KO mice and therefore, motor learning could be impaired (Sakurai 1990; Kano et al. 1992). However, in the Rota Rod task Mena KO mice have shown similar improvement in performance to WT animals, suggesting that Mena is not essential for motor learning.

To obtain a more complete phenotype of the Mena KO mice I also investigated the stress response performing the tail suspension test. Measurement of the immobility time in this task revealed that Mena KO mice are significantly less prone to despair and therefore less sensitive to this type of stress. However, in order to provide conclusive data about this issue other tests, such as forced swimming test, measurement of the social interactions in aversive environment or the elevated zero-maze, will have to be performed.

Finally, since the hippocampal commissure is involved in learning and memory and the disruption of the Mena gene has been shown to cause abnormalities in the corpus callosum and hippocampal commissure (Lanier et al. 1999), I performed the operant task in order to address the role of Mena in these processes (2.2.15). Measuring the number of operative (correct) responses accomplished by the animals during the test session, Mena KO showed less correct responses when compared to WT mice. To exclude a general lower activity of Mena KO mice during the test session, I compared the number of the inoperative (incorrect) responses produced by Mena KO and WT littermates. No difference between Mena KO and WT animals was observed in this respect. Therefore I can conclude that lack of Mena impairs the processes of learning and decreases

memory, however further analyses need to be performed to evaluate fully the involvement of Mena in these higher brain functions.

Common pathways of profilin2 and Mena *in vivo?*

For actin cytoskeleton reorganization the physical interaction between Mena and profilins might be important. In mice, 50% reduction of profilin1 in Mena null background leads to embryonic lethality due to defects in neuronal tube closure (Lanier et al. 1999). The majority of reports concerning the functional relationship between Mena and profilin comes from the invertebrate *Drosophila*, that carries only one profilin gene (*chickadee*). Therefore the identification of the brain specific profilin2 in mice enables the exploration of the specific role played by Mena in modulating of the actin cytoskeleton through a more complex profilin prism. Mena has been shown to associate with profilin2 in brain, however the significance of this interaction *in vivo* is not clear (Witke et al. 1998). In order to address the functional interaction between profilin2 and Mena I compared the neuronal cell phenotype and the behavior of mice where either Mena or Profilin2 gene was knocked-out (Profilin2 KO mice were analyzed by Alessia Di Nardo and Pietro Pilo Boyl, Witke laboratory).

Comparative analysis of the morphology displayed by Mena and profilin2 KO hippocampal neurons revealed that both KO cells spread quicker after plating and produce longer primary processes than WT cells, suggesting a faster development. Both Mena and profilin2 KO mice show significant alterations in locomotor activity. While Mena KO mice are less active, profilin2 KO mice exhibit 2-3 times higher activity than WTs in the open field test. Locomotion is generally linked to the basal ganglia and to the upstream dopaminergic system. Lower activity observed in Mena KO mice might result from less dopamine inputs reaching the striatum or from impairments in the signal transmission within GABAergic neurons in the basal

ganglia. Recent work showed that Mena, profilin and gephyrin colocalize at inhibitory (GABAergic) synapses of rat spinal cord and at gephyrin clusters generated in transfected cells (Giesemann et al. 2003), suggesting that they are probably involved in neurotransmission. Lack of Mena might lead to impairments in clustering of the GABA receptors and therefore lower locomotor activity. However, an explanation for the opposite phenotype found in profilin2 KO mice and a common functional pathway for Mena and profilin2 requires further investigation using neurophysiological methods such as tissue neurotransmitter content, *in vivo* microdialisis and electrophysiology. Profilin2 KO mice, similarly to Mena KO mice displayed impairments in the motor coordination and balance. In addition both KO models showed reduced grip strength.

Locomotor activity, coordination and balance are strongly age-dependent in both Mena and profilin2 KO mice. Interestingly, about 50% of the profilin2 KO mice die between the age of 6-10 months, apparently by paralysis. Analysis performed on muscles of these animals revealed the absence of neuromuscular junctions. There is some evidence that profilin2 might be important in vesicle trafficking, resulting in a disregulation of neurotransmitter release or reuptake. This may lead to over-stimulation of neurons in striatum or spinal cord and therefore neurodegeneration in the long term, which can explain the death by paralysis of profilin2 KO mice and the observed loss of neuromuscular junctions. Analysis addressing this issue in Mena KO mice remains to be completed.

Finally, lack of profilin2 and Mena seems to affect the stress response, however in order to specify what type of stress response is involved and whether in both cases the outcomes are similar further investigation needs to be performed.

Comparison of the behavior of profilin2 and Mena KO mice as well as the morphology of the hippocampal neurons shows a remarkable overlap. This might indicate the existence of common pathways where both profilin2 and Mena act that lead to a similar readout in terms of behavior. However further behavioral and

neurophysiological investigations are needed. Combining and studying both mutations *in vivo* by generating a double KO mice would be one of the best directions to follow.

4. Material and Methods

4.1 Molecular Biology

4.1.1 Cloning strategy used for targeting of the human profilin1/profilin2 cassette into profilin1 locus.

Generation of IRES human P1/P2 targeting construct

pIRES-FLRT-A plasmid was used as a base for generating IRES hP1/P2 targeting construct (plasmid # 267, Witke archive).

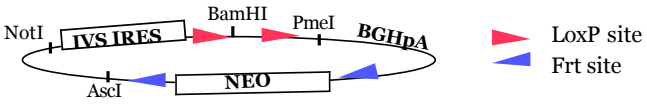

pIRES-FLRT-A

Sub-cloning of human profilin1 cDNA was performed by PCR amplification of human profilin1 coding region from parental cDNA (plasmid # 301, Witke archive) using the following pair of primers:

*Bam*HI *Eco*RI
HP1FOR: 5'-GATCG**GATCCGAATTC**AGCGCCATGGCCGGGTGGAACGCCTAC–3'
*Bam*HI
HP1REV: 5'-GATC**GGATCC**TCAGTACTGGGAACGCCGAAGGT–3'

The reaction was carried out in 50μl total volume composed of: 1× PCR buffer (Promega), 1.5mM MgCl2, 200nM dNTPs, 100nM oligos, 5 units of TaqPol (Promega). The PCR fragment was subsequently digestested with the BamHI endonuclease and ligated into the pIRES-FLRT-A plasmid, BamHI digested.

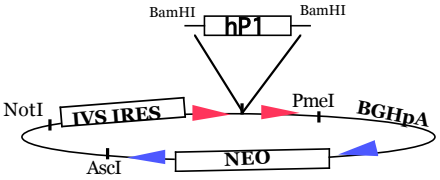

pIRES-FLRT-A–hP1

In the next step, a PmeI fragment containing mouse profilin2 cDNA from parental plasmid #32 (Witke archive) was ligated into PmeI digested the pIRES-FLRT-A-hP1 plasmid, downstream of hP1 and upstream of the bovine growth hormone 3'UTR polyadenylation signal (BGHpA).

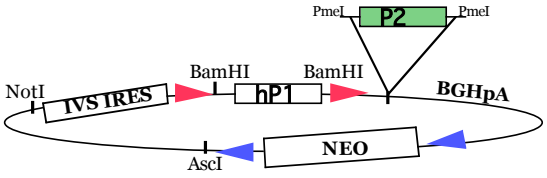

pIRES-FLRT-A-hP1/P2

The purpose of this cloning was to generate the cassette containing IRES-hP1/P2pA followed by the NEO resistance cassette flanked with Frt sites.
The NA9 plasmid carries a fragment of the profilin1 genomic locus. In order to facilitate the subsequent cloning steps, a DNA linker including a stop codon and restriction sites for *Not*I and *Asc*I was introduced into the *Nco*I site of NA9 plasmid, which overlaps the profilin1 start codon (ATG). This modification switches off the profilin1 wild type locus.

Sequences of the STOP-*Not*I-*Asc*I linker:

STOP *Not*I *Asc*I
STOP-*Not*I-*Asc*I sense: 5'-CATG**TAAGCGGCCGC**GAAC**GGCGCGCC**-3'

*Asc*I *Not*I STOP
STOP-*Not*I-*Asc*I antisense: 5'-CATG**GGCGCGCC**GTTC**GCGGCCGCTTA**-3'

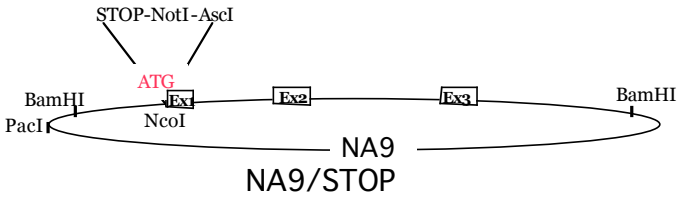

The IRES-hP1/P2-NEO cassette was recovered from pIRES-FLRT-A-hP1/P2 plasmid as a NotI-AskI fragment of 4.2kb and cloned into NA9/STOP plasmid. Before ES cells transfection the targeting vector for the replacement experiment of profilin1 by profilin2 was linearized with PacI.

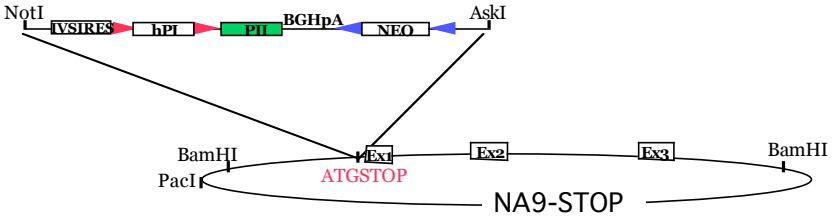

NA9-IRES-hP1/P2-NEO targeting vector

NA9-IRES-hP1/P2-NEO targeting construct was subjected to restriction analysis in order to confirm the expected modification in profilin1 locus.

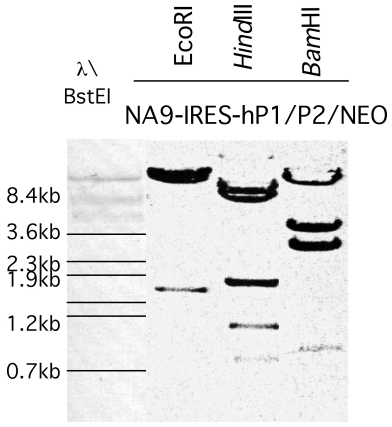

Figure 24 Confirmation of the presence and position of expected restriction sites in NA9-IRES-hP1/P2-NEO targeting construct.
NA9-IRES-hP1\P2-NEO targeting vector was subjected to restriction digest with *EcoR*I, *Hind*III and *Bam*HI endonucleases. All the sites are correctly localized.

4.1.2 Cloning strategy used for targeting proflin2 cDNA into profilin1 locus.

Generation of the Profilin2 cDNA targeting construct

The purpose for generating the following targeting construct was to enable expression of profilin2 gene under control of profilin1 promoter, obtained by direct fusion of profilin2 coding sequence to the ATG (start codon) of profilin1.

Profilin2 cDNA was generated by PCR amplification on the parental plasmid carrying the coding sequence for profilin2 (plasmid #32, Witke archive). Reaction was performed using the following pair of primers:

*Nco*I
P2NcoI: 5'-GCAGC**CCATGG**CCGGTTGGCAGAGC-3'
*Nco*I*Xho*I
P2XhoI-NcoI: 5'-GCTCA**CCATGGCTCGAG**CTAGAACCCAGAGTCTCTC-3'

Introduction of the suitable restriction sites into profilin2 cDNA fragment, during PCR amplification, makes profilin1 locus accessible for further modifications. Because of the presence of an endogenous *Nco*I site in 3' of profilin2 coding sequence, the generated PCR fragment was subjected to partial restriction digest with *Nco*I endonuclease and cloned into NA9 plasmid *Nco*I digested.

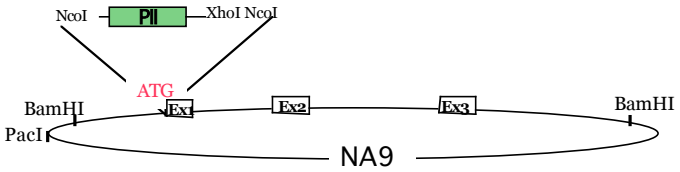

NA9-P2cDNA

In order to enable expression of profilin2 coding sequence as well as the selection of targeted ES clones, the cassette composed of bovine growth hormone 3'UTR and polyadenylation signal (BGHpA) followed by the NEO resistance gene flanked with Frt sites was cloned in NA9-P2cDNA plasmid *Xho*I digesed.

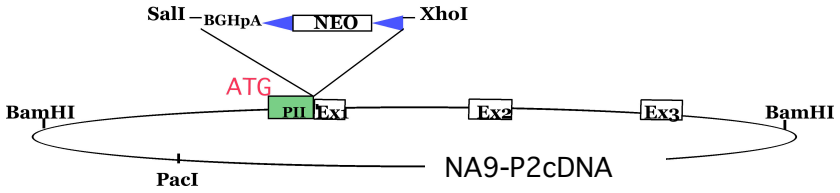

NA9-P2cDNA-NEO

Before ES cells transfection the targeting vector was linearized with *Pac*I.

NA9-P2cDNA-Neo targeting construct was subjected to restriction digest in order to confirm the expected modification of profilin1 locus.

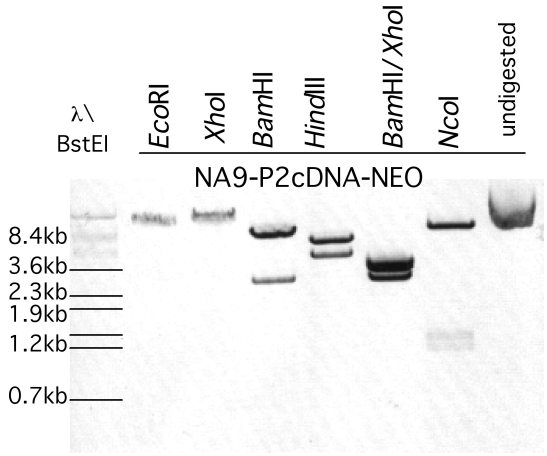

Figure 25 Restriction analysis of the NA9-P2cDNA-NEO targeting vector.
Resulted restriction pattern confirmed correct localization of all the sites examined (*EcoR*I, *Xho*I, *Hind*III, *Bam*HI and *Nco*I).

4.1.3 Validating the recombinase recognition sites by transfections of Cre and Flp expressing bacteria with NA9-IRES-hP1/P2-NEO and NA9-P2cDNA-NEO targeting constructs

In order to determine functionality of Frt and LoxP sites present in the targeting constructs, E.coli bacteria that carry FLP or CRE recombinase gene as an insertion into their genome were subjected to electroporation with NA9-IRES-hP1/P2-NEO and NA9-P2cDNA-NEO targeting constructs. Plasmid DNA isolated from bacteria upon the transfection was analyzed for the proper deletion.

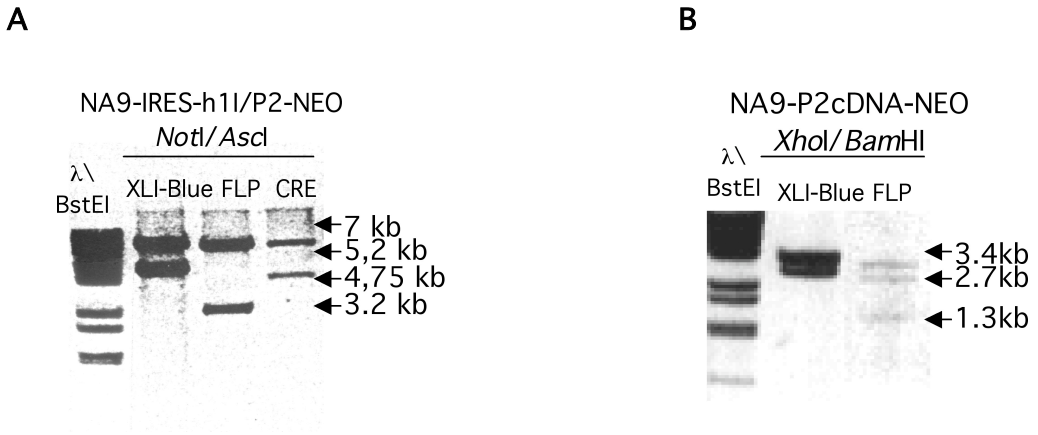

Figure 26 Determination of the validity of the recombination recognition sites by transformation of the targeting vectors: NA9-IRES-hP1/P2-NEO and NA9-P2cDNA-NEO into Cre and Flpbacteria.
A) Diagnostic digest of NA9-IRES-hPI/PII-NEO targeting construct with *Not*I and *Asc*I endonucleases illustrating deletion of NEO cassette and human profilin1 cDNA after homologous recombination that occurred in FLP and CRE expressing bacteria.
B) Diagnostic digest of NA9-PIIcDNA-NEO targeting construct with *Xho*I and *Bam*HI endonucleases illustrating expected deletion of NEO cassette after homologous recombination in FLP expressing bacteria.

4.1.4 Genomic DNA isolation from mouse-tail biopsy and PCR analysis of mutant mice

Mutant mice were genotyped by PCR analysis using specific primers. Genomic DNA was prepared from a 0.5 cm tail biopsy, taken from 3-weeks old pups, after over night digestion in 200μl of DNA lysis buffer (50 mM Tris-HCl, pH 7.5, 100 mM NaCl, 5 mM EDTA, 1% SDS) with 100 μg/ml of proteinase K at 55°C. After the

lysis, genomic DNA was extracted by virgorous mixing with half volume of saturated NaCl and centrifugated 10 minutes 14x10^{3}rpm. Genomic DNA was precipitated from the supernatant with 2,5 volume of absolute ETOH, dried and resuspended in 300µl of sterile water. The following primer combinations and PCR programs were used to identify mutations of interest:

Mena knock-out mice

GTF: 5'-AATCGCACACTCTGTCCATATTCC-3'
GTR: 5'-TGCCCACAACTCTGAATGTGTTG-3'
BGR: 5'-TCCCAGTCACGACGTTGTAAAAC-3'

MENA-PCR
Step 1) 98°C 2:00
Step 2) 96°C 0:30
Step 3) 55°C 1:30
Step 4) 72°C 0:30
Step 5) back to step 2) 34x
Step 6) 72°C 5:00

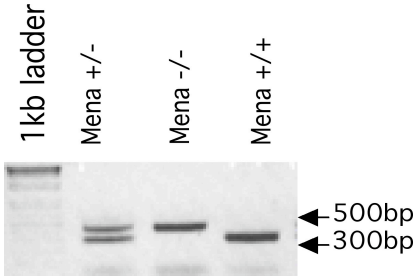

Expected PCR products: 500bp mutant band, 300bp wild type band.

Profilin2 knock-out mice

NestPllfor: 5'-TCCATTCTGGAGACATAATGG-3'
NestPllrew: 5'-CAATGCTGGAGTACACAAGG–3
NestLacZ: 5'–CTGCAAGGCGATTAAGTTGG–3'

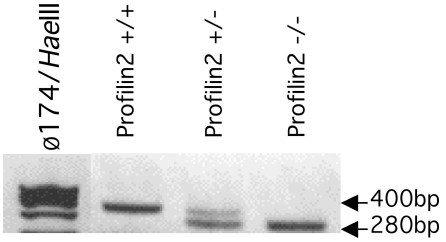

Profilin2-PCR
Step 1) 98°C 2:00
Step 2) 96°C 0:30
Step 3) 55°C 1:15
Step 4) 72°C 0:30
Step 5) back to step 2) 34x
Step 6) 72°C 5:00

Expected PCR products: 280bp mutant band, 400bp wild type band.

FLP- recombinase transgene

SD222: 5'-CCCATTCCATGCGGGGTATCG-3'
SD223: 5'-GCATCTGGGAGATCACTGAG-3'

FLP-PCR
Step 1) 98°C 2:00
Step 2) 90°C 1:00
Step 3) 65°C 1:00
Step 4) 72°C 0:30
Step 5) back to step 2) 30x
Step 6) 72°C 7:00

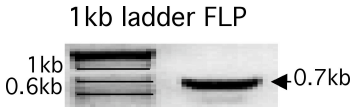

Expected PCR product: 700bp. FLP- recombinase band.

CRE-reombinase transgene

CRE1: 5'-GCCTGCATTACCGGTCGATGCAACGA-3'
CRE2: 5'-GTGGCAGATGGCGCGGCAACACCATT-3'

CRE-PCR
Step 1) 94°C 2:00
Step 2) 94°C 0:30
Step 3) 55°C 0:30
Step 4) 72°C 0:40
Step 5) back to step 2) 30x
Step 6) 72°C 5:00

Expected PCR product: 550bp. CRE recombinase band.

IRES-hP1/P2-NEO knock-in allele

(HP1FOR) #1: 5'-CGAATTCAGCGCCATGGCCGGGTGGAACGCCTAC-3'
(HP1REV) #2: 5'-GATCGGATCCTCAGTACTGGGAACGCCGAAGGT-3'

Human P1-PCR
Step 1) 98°C 2:00
Step 2) 94°C 0:30
Step 3) 71°C 0:45
Step 4) 72°C 1:00
Step 5) back to step 2) 30x
Step 6) 72°C 7:00

Expected PCR product: 430bp. human profilin1 band.

Profilin2 cDNA knock-in allele

(FRTREV) #5: 5'-CCTATTCTCTAGAAAGTATAGC–3'
(MP2AFOR)#6: 5'-CAGGATCCATGGCCGGTTGGCAGA–3'

Profilin2cDNA/BGHpolyA-PCR
Step 1) 98°C 2:00
Step 2) 96°C 0:30
Step 3) 60°C 1:30
Step 4) 72°C 0:30
Step 5) back to step 2) 34x
Step 6) 72°C 5:00

Expected PCR product: 730bp. profilin2 cDNA/BGHpA band.

4.1.5 Genomic DNA isolation from ES cells and Southern blot analysis

To prepare genomic DNA from ES cells, cells were grown to confluency without feeder layer in 12 well dishes (Falcon) and lysed by overnight digestion at 37°C in 0,5 ml of DNA lysis buffer (Laird et al.1991)(100mM Tris-HCl, pH 8,5, 5 mM EDTA, 0,2% SDS, 200 mM NaCl) with 100μg/ml of proteinase K. The next day genomic DNA was precipitated by adding 1 volume of isopropanol, and gentle mixing on the gyrator shaker, washed in 70% ETOH, dried and resuspended in 100μl of 1xTE buffer.
For Southern blot assay 10 μg of genomic DNA were digested with the appropreate restriction enzyme and separated on a 0,7% agarose gel. DNA fragments were carried on upward in a flow of alkaline buffer and were deposited onto the surface of a charge nylon membrane (Gene Screen Plus NEF 976). After the transfer the membrane was baked at 80°C for 1 hour and afterwards pre-incubated in hybridization buffer (1% BSA, 1 mM EDTA, 0,5 M Na-phosphate

buffer pH 7.2, 7% SDS) at 65°C for 30 minutes. DNA probes were labeled by random priming with [^{32}P]α-dGTP (Feinberg and Vogelstein 1983), added to fresh hybridization buffer and allowed to hybridize membrane over night at 65°C. Next day filters were washed four times in wash buffer (1mM EDTA, 40mM Na - phoshate buffer pH 7.2, 1% SDS) at 65°C and exposed to autoradiographic film over night or longer at -80°C.

4.2 Cell biology

4.2.1 ES cells cultures and transfection

IB10 embryonic stem (ES) cells were derived from 129sv blastocysts. ES cells were grown on an embryonic fibroblast feeder layer (EF-feeders) plated on 0.2% gelatin coated dishes in DMEM containing 15% fetal bovine serum, 2mM L-glutamine, 0.1 mM nonessential amino acids, 0.1 mM β-mercaptoethanol (Sigma), 100 u/ml penicillin/streptomycin mixture, 1000 u/ml leukemia inhibitory factor (LIF) at 37°C and 5% CO_2.

4.2.1a ES cells transfection

Before transfection, cells were washed twice in PBS buffer, harvested by tripsinization and after washing in electroporation buffer (10mM HEPES buffer in DMEM without FCS) resuspended at 1x 10^7 cells/ml in a final volume of 0.7 ml. Cell suspension was electroporated using BioRad Gene Pulser set at 250 V/cm and 500μF for one pulse at RT. 30μg of linearized plasmid DNA was used for one transfection. After pulsing, cell suspension was diluted in 10 ml of complete medium and plated on 10 cm dishes. Selection started 1 day after transfection in 0.25 mg/ml G418.

4.2.1b ES cell clones selection

After having reached visible size, single ES cells clones were picked and expanded in 24 or 96 well plates on EF-feeders in selection medium. Once reached a confluence of 70-80%, ES cells were harvested and for every well 50% was used for freezing back up aliquots while the remaining 50% was further expanded on

0.2% gelatin coated dishes for genomic DNA extraction Screening of the ES cells clones for homology recombination event was performed by Southern Blot.

4.2.2 Neuronal primary cultures and *in vitro* neurodegeneration assays

Pregnant females were sacrificed on day 16 of gestation. The embryos were collected for primary neuronal cultures as described in section. 4.2.1a. The primary cultures were used to study neurite outgrowth of embryonic hippocampal neurons and cell susceptibility to apoptosis and necrosis in *in vitro* neurodegeneration assays of cortical neurons.

4.2.2a Cortical and hippocampal neurons primary culture

On day 0 of the experiment, E16.5 mouse embryos were collected in 1x Tyrode's solution (NaCl – 8 g/L; KCl – 0.2 g/L; $MgCl_2x6H_2O$ – 0.1 g/L; $NaH_2PO_4xH_2O$ – 50 mg/L; $NHCO_3$ - 1 g/L; Glucose – 1 g/L; all chemicals were purchased from Sigma, St. Louis, MO). The brains were removed and both cortex and hippocampi were dissected out and collected separately in 1x Ca^{2+} and Mg^{2+}-free Tyrode's solution (NaCl – 8 g/L; KCl – 0.3 g/L; $KH_2PO_4xH_2O$ – 25 mg/L; $NaH_2PO_4xH_2O$ – 50 mg/L; $NHCO_3$ - 1 g/L; Glucose – 2 g/L; all chemicals were purchased from Sigma, St. Louis, MO). The tissue was cut into small pieces and incubated with 0.2 % Trypsin (Sigma, St. Louis, MO) for 15 min at 37°C. The trypsinization reaction was stopped by adding a 10 % fetal calf serum medium (MEM Earle's salts (Gibco BRL, Rockville, MD) containing 100 μg/ml penicillin/streptomycin mixture and 0.125M Glucose). The suspension was then treated with DNaseI (0.5 mg/ml; Worthington, Lakewood, NJ) and cells were dissociated by trituration with a Pasteur pipette. Dissociated hippocampal cells were resuspended in a Neurobasal medium containing Penicillin/Streptomycin (100 μg/ml, Gibco BRL, Rockville, MD), L-Glutamine (0.292 mg/ml, Gibco BRL, Rockville, MD), serum-free B-27 supplement (Gibco BRL, Rockville, MD). The cell density was determined and the preparation was diluted to a density of $3x10^4$ cells/ml with the above neurobasal medium and plated on cover slips (BDH 19 mm,thickness #1) coated with poly-DL-Ornithine bromamide (Sigma) for neurite outgrowth assay. The cortex preparation was also diluted to 5 or 10 $x10^4$ cells/100 μl with the above neurobasal medium containing 10 % fetal calf serum, dependending on the following neurodegeneration assay. Cell suspensions (100 μl/well) were plated on pre-soaked Poly-L-Ornitine/Laminin 96-well plates (Becton Dickinson, Bedford MA) and placed at 37 °C in a 5% CO_2 incubator.

4.2.2b Determination of neurite growth by digital image analysis

Mouse hippocampal neurons were prepared and plated as described in section 4.2.2a. For the neuronal differentiation process four time points were taken into consideration performing the study on neurite outgrowth: 6, 24, 48 and 72 hours after plating. At each time point neurons were fixed in 4% paraformaldehyde (PFA) for 15 min, RT and subjected to immunofluorescent staining procedure as described in section 4.2.2c. In order to determine parameters reflecting neurite outgrowth, images of neurons were captured at the appropriate wavelength by Leica DC500 digital camera attached to Leica DMR microscope. Images were analyzed with freehand line and freehand area selection options of ImageJ software, statistical analysis of the collected data was performed with two-way analysis of variance (ANOVA) for repeated measures.

4.2.2c Immunostaining of hippocampal neurons

Neurons were fixed in 4% paraformaldehyde (PFA) for 15min, RT. Aldehyde groups were quenched in 50 mM amonium chloride for 10 min and the cells were extracted with 0,1% TritonX-100 for 2 min. The neurons were blocked in blocking solution (2% FCS, 2% BSA, 0.2% fish gelatin in PBS) for 30 min, RT. Incubations with primary and secondary antibodies were performed in antibody solution (10% blocking solution, 0.5% FCS in PBS) for 1h and 30 min respectively.
The following dyes and primary antibodies were used for immunostaining performed on hippocampal neurons:
TRITC- conjugated phalloidin (Molecular Probes, Leiden, Netherlands), anti- βIII tubulin (Promega), anti-Tau1 (Roche) anti-MAP2 (Sigma).
The secondary antibodies used were: rhodamine (TRITC)-conjugated AffiniPure goat anti-mouse (Jackson ImmunoResearch Laboratories, Inc., 1.4 mg/ml) and fluorescein (FITC) conjugated AffiniPure Goat Anti-mouse (Jackson ImmunoResearch Laboratories, Inc.) Detailed information about dilution used for different assays is found in Table 5, section 4.3.2. Images were viewed with a Leica DMR microscope equipped with epifluorescence.

4.2.2d *In vitro* neurodegeneration assays

In order to assess cell viability during apoptosis and necrosis embryonic cortical neurons were subjected to *in vitro* neurodegeneration assays. The experimental design is outlined in the diagram below.

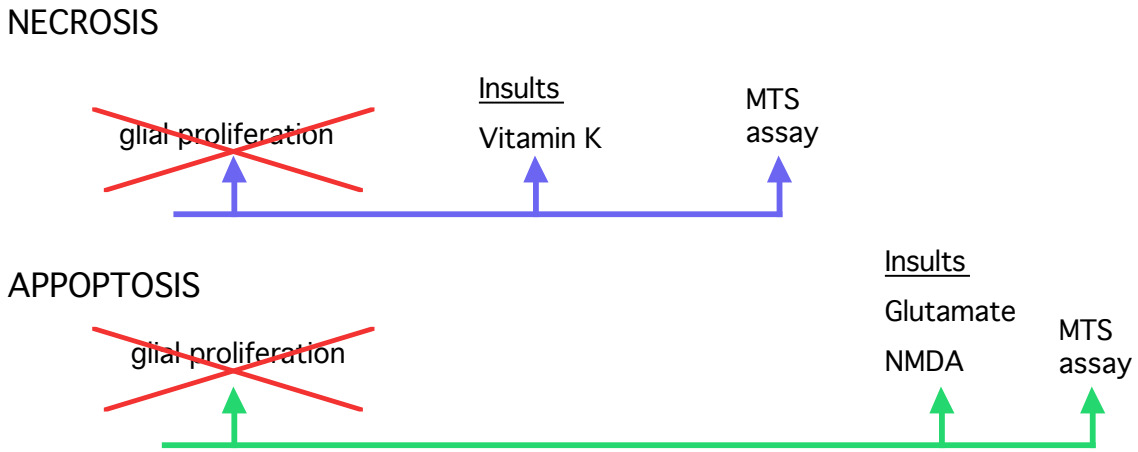

Cortical neurons were prepared and plated as described in section 4.4.2a. Cells to assess necrosis by applying vitamin K (25 μM) were plated at a 5 x 10^4 cells per well density. Cells used to assess glutamate (10 and 30 μM) and NMDA (30 and 100 μM) toxicity due to apoptotic cell death were seeded at a density of 10 x 10^4 cells per well.

4.2.2e Cytosine arabinoside treatment

After 2 days in culture, neurobasal serum-free medium (50,000 cells per well plating) and neurobasal medium containing 10% fetal calf serum (100,000 cells per well plating) were replaced by neurobasal serum-free medium containing cytosine arabinoside (Ara-C, 10 μg/ml, total volume 200 μl (Sigma, St. Louis, MO), to prevent astrocytes proliferation.

4.2.2f Oxidative stress - Menadione insults

The necrosis assays were performed on 50,000 cells/well density plates on day 4. Treatment of cultures with the sodium bisulfite adduct of Menadione for 48 hours was used as an oxidative stress paradigm. Menadione was added at a final concentration of 25 μM and cells were incubated at 37 °C for 48hrs; afterwards cell viability was assessed as described in section 4.4.2h.

4.2.2g NMDA-Glutamate-insults

Glutamate and NMDA insults were performed on 100,000 cells/well density plates on day 8 of the experiment as described in (Schubert and Piasecki 2001). On day 8 of the experiment the medium was removed from the primary neuronal cultures and saved in a new 96-well plate. The cells were treated with glutamate (5, 10 and 30 μM) or NMDA (10, 30, 100 and 500 μM) in the HCSS buffer (120 mM NaCl, 5.4 mM KCl, 0.8 mM MgCl2, 1.8 mM CaCl2, 15 mM glucose and 20 mM HEPES, pH 7.4) or with HCSS alone for 10 min at room temperature. Then the HCSS was aspirated and the original growth medium was returned to the cells. The effects of glutamate and NMDA were compared to those of HCSS alone. Cell viability was evaluated 3 hrs and/or 48 hrs after drug application as described in section 4.4.2h.

4.2.2h Determination of cell viability via MTS

Cell viability was evaluated by CellTiter 96 Aqueous One Solution Cell Proliferation Assay (Promega Corporation, Madison, WI). This assay is based on conversion of MTS tetrazolium compound into a colored formazan product that is soluble in cell culture medium. Assays are performed by adding 20 μl of CellTiter 96 Aqueous One Solution reagent directly to culture wells, incubating for 3 hours and then recording absorbance at 490 nm with a 96 well plate reader. The quantity of formazan product measured by absorbance at 490 nm is directly proportional to the number of living cells in the culture.

4.3 Biochemistry

4.3.1 Preparation of protein lysates from cell lines and mouse tissues for western blot analysis

4.3.1a Primary hippocampal neurons and ES cells lysates

Cells were grown in 6 and 12 well plate dishes, coated with poly-DL-Ornithine bromoamide (0,5 mg/ml) and gelatin (0.2%) respectively. At 70-80% confluence cells were washed two times with 1x PBS buffer and mechanistically removed from the culture dishes directly into 1x SDS sample buffer (22 mM Tris-HCl pH 6.8, 0.8% SDS, 4% glycerol, 1.6% β-Mercaptoethanol, Bromphenolblue). The protein lysate is obtained boiling for 10 min 95°C.

4.3.1b Tissues lysates

In order to prepare tissue lysates, dissected mouse organs were placed in PEB buffer (20mM Tris-HCl, pH 8.0, 100 mM NaCl, 5mM EGTA, 2 mM EDTA, 0,2% Tween-20, 0.5 μM APMSF), and dissociated using a douncer. Lysates were centrifuged for 45 min at 65.000 x rpm at 4 °C Clear supernatant were transferred into the fresh tubes and aliquots were boiled with SDS sample buffer.
Protein concentration in the extracts was determined with the Bradford reagent (BioRad).

4.3.1c Western blot analysis

For SDS-PAGE, proteins were diluted in 1x SDS sample buffer, denatured by heating 10 min at 95°C and subjected to gel electrophoresis. Proteins were electrophoretically transferred onto a polyvinylidene difluoride (PVDF) membrane (Immobilon-P, Millipore) using a semi-dry apparatus by applying 20V for 1h. Gel and membrane were equilibrated in transfer buffer (25 mM Tris, 190 mM Glycine, 20% Methanol pH 8.3) before transfer. After the transfer membrane was incubated in blocking solution (5% non-fat powder milk dissolved in NCP buffer (0.15 M NaCl, 20 mM Tris, 0.05% Tween-20) at 4 °C overnight. Primary and secondary antibodies were diluted in blocking solution to the appropriate concentrations. To detect the signal between the antibodies incubations, the membranes were washed 5 times in NCP buffer. The enhanced chemiluminescence

system (Amersham) was used followed by the exposure to x-ray films (X-Omat AR, Eastman Kodak Co).

4.3.2 Primary and secondary antibodies used for western blot and immunochemistry assays

The following primary antibodies were used: anti-Mena, anti-profilin2A, anti-profilin1, anti-actin. For detection, horseradish peroxidase (HRP) conjugated secondary goat anti-rabbit and goat anti-mouse antibodies (Pierce). Detailed information regarding specificity and concentration of the antibody used in the assays is contained in Table 6.

Primary antibody	Specificity	Description	Company	Assay and used dilution
anti-Mena	80 and 140kDa mouse human Mena	N-term rabbit polyclonal	Witke Lab	Immuno-staining 1:200 WB 1:1000
3003ab	mouse profilin 2A	peptide - rabbit polyclonal	Witke Lab	WB 1:1000
anti-profilin1	mouse profilin 1	rabbit polyclonal	Witke Lab	WB 1:1000
anti-actin	mouse,human, bovine β-actin	monoclonal clone # AC-74	Sigma	WB 1:500
2H11ab	human, bovine profilin1	mouse monoclonal	Jokusch Lab	WB 1:1000
anti-Tau1	mouse, human bovine	mouse monoclonal # PC1C6	Roche	Immuno-staining 1:200
anti-MAP2	mouse, rat, human MAP2	mouse monoclonal	Sigma	Immuno-staining1:5000
anti-βIII tub	mouse, rat βIII- tubulin	monoclonal clone #5G8	Promega	Immuno-staining1:500
anti-GFP	Wt GFP, EGFP	Recombinant rGFP E.coli	Clontech	WB 1:2000

Secondary antibody	Specificity	Description	Company	Assay and used dilution
Rhodamine ab	goat anti mouse	TRITC-conjugated	Lackson ImmunoResearch Lab.	Immuno-staining1:1000
Fluorescein ab	goat anti mouse	FITC-conjugated	Lackson ImmunoResearch Lab.	Immuno-staining1:1000
Horse radish peroxidase ab	goat anti mouse	HRP-conjugated	Pierce	WB 1:1000
Horse radish peroxidase ab	goat anti rabbit	HRP-conjugated	Pierce	WB 1:1000

Table 6 Collection of primary and secondary antibodies that were used for immunostaining and western blot assays.

4.3.3 List of dyes used for immunochemistry assays

Alexa™ 488-Phalloidin (FITC) 200u/ml, 1:200 dilution
Alexa™ 594-Phallodin (TexasRed) 200u/ml, 1:200 dilution
Hoechst 33342, 10ng/ml, 1:30000 dilution

All products were purchased from Molecular Probes Europe BV.

4.4 Mice

The following mutant mice were used in this work.

4.4.1 Mena KO mice

Mena mice were a kind gift of Frank Gertler (Departement of biology, Massachusetts Institute of Technology, Cambridge Massachusetts)

A targeted disruption of the Mena locus was generated through homologous recombination in AK7 ES cells (Imamoto and Soriano 1993). The β-geo cassette with a polyadenylation signal (Friedrich and Soriano 1991) followed by the neomycin cassette replaced exons 2 and 3 of the Mena gene. The resulting locus produces a fusion protein containing 5' untranslated region of Mena and the initiating methionine fused in frame to β-geo cassette. The cloning strategy leads to a Mena protein null mutant and the expression of LacZ reporter gene under the control of the endogenous Mena promoter. Correctly targeted clones were identified by PCR and verified by Southern blot analysis. Germline transmission of the disrupted allele was verified by PCR and Southern blot analysis. Mena mice were genotyped by PCR as described section 4.1.4.

4.4.2 Profilin2 KO mice

Conventional Profilin2 knock-out mice were generated by Alessia di Nardo (Witke laboratory, EMBL- Monterotondo).

In order to disrupt profilin2 locus the β-gal-PGK NEO cassette was introduced into the exon 3 of profilin2 gene resulting in a profilin2 null allele. The targeting vector was electoporated into J1 embryonic stem cells. Correctly targeted clones identified and confirmed by Southern blot and PCR analysis were injected into

C57Bl/6 blastocysts as described (Friedrich and Soriano, 1991). Western blot analysis confirmed lack of profilin2 expression. P2 KO mice were genotyped by PCR using a pair of specific primers, as described in section 4.1.4.

4.4.3 Housing condition of the animals used for primary behavioral phenotyping

Mice were single housed for one week before the performance of the behavioral tests and remained in such a housing condition until the end of the experiments. Animals were housed at a 12 hours light-dark cycle (8am-8pm) and at constant humidity maintained at 55% in the rooms devoted for Phenotyping Core Facility, Mouse Biology Program, EMBL – Monterotondo. Food and water were supplied *ad libitum*.

4.5 Behavioral analysis

4.5.1 Infra Mot – exploratory activity in the home cage

TSE InfraMot (Technical & Scientific Equipement GmBH) is a system for determination of circadian and locomotor activity of the mice in their home cage environment (Figure 27)

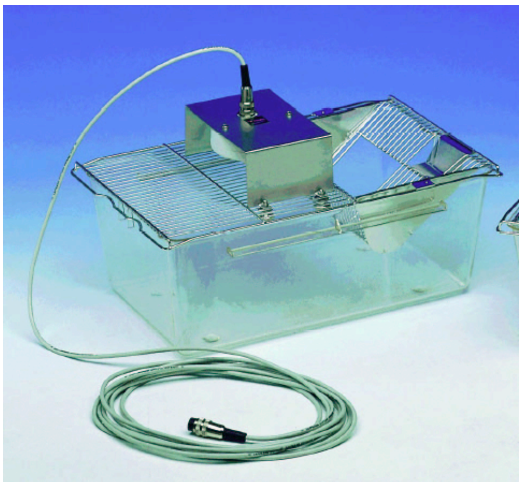

Figure 27 TSE Infra Mot apparatus – measurement of exploratory activity of the small laboratory animals in their home cage.

The system uses so called “passive infrared sensors”. These sensors register the activity of a subject by sensing the body-heat image by the emitted infrared radiation and its displacement over time. In this way movement in the cage can be reliably determined. The sensors were assembled on top of animals’ home-cage. The entire recording session lasted for 24 hours over 5 consecutive days. Measurements were taken every 5 min. Infra Mot data were analyzed using a two-way ANOVA for repeated measures (Statview 5.0, Abacus Concept, USA).

4.5.2 Open Field – measurement of the locomotory activity

The most standardized general measure of motor function is spontaneous activity in the open field (Figure 28). A group of 31 animals (Table 3) was subjected to a one-hour open field test under standard room light conditions during the light phase of the circadian cycle. Each session was video recorded. The camera was placed above four separate open field areas (white, round, 60 cm diameter, made of formica), which enables for simultaneous record of four animals at the time.
Activity in the open field was quantified using TSE VideoMot 2 (Technical & Scientific Equipment GmbH) computer software. The activity measuring system calculates a number of relevant variables: total distance traversed, total number of movements, time spent in the center of the open field (represents 40% of the surface of the open field) versus time spent in the periphery of the field and time spent in certain user-defined areas of the open field. The results were stored as ASCII file for further statistic evaluations.

A B

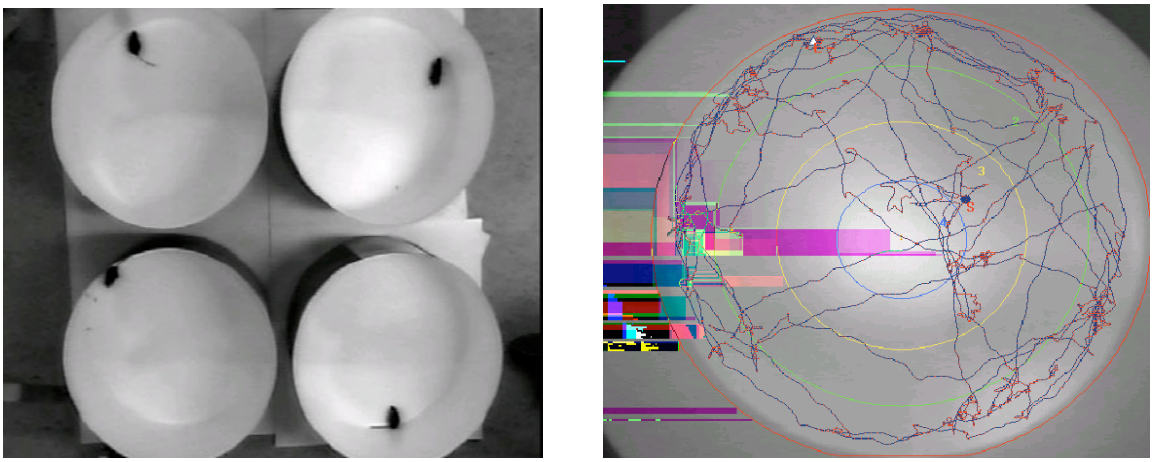

Figure 28 Open field apparatus – measurements of the locomotory activity
A) Setting of the four open fields for parallel video recording. **B)** Computer analysis of the locomotor activity of the mouse traced in the open field test.

Open field data were analyzed as follows: distance traveled over 5 min periods (two-way ANOVA for repeated measures), total path traveled in 60 min. (one-way ANOVA) as well as time spent and distance traveled in the center of the open field (one-way ANOVA). Open field areas were cleaned after each round with 10% ETOH, which prevents the next mouse from being influenced by the odors deposited in the urine and the feces of the previous mouse.

4.5.3. Rota Rod – motor coordination, balance and motor learning

Rota Rod is the behavioral task used for measuring motor coordination, balance as well as motor learning. The mouse placed in the Rota Rod apparatus (Figure 29,TSE Technical & Scientific Equipment GmbH) must continuously walk forward to keep from falling off the rotating bar. Fifteen minutes before the performance of the task mice were transferred to the experimental room in order to habituate them to the environment. The experimental room environment was maintained constant between the sessions with respect to temperature, humidity and light intensity. A group of 31 animals (Table 3) was subjected to the test. Five mice at the time, blindly chosen with respect to genotype, were placed in rotating units and the apparatus started turning. Three training trials of 60 seconds were performed as follows:

1) 0 rpm for 60 seconds
2) 4 rpm constant speed for 60 seconds
3) 4 rpm constant speed for 60 seconds

The pause in between training trials and the test was 30 minutes. The Rota Rod test was composed of four consecutive sessions. During the test sessions rotating speed was gradually increased over a 5 minutes period according to a predetermined program ramping up from 4 rpm to a maximum rotation speed of 40 rpm. Latency of falling off the rotating drum as well as rotating speed were recorded and used as a quantitative measurement of motor coordination and balance of the animals. Rota Rod data were analyzed using one-way ANOVA. After each session the apparatus was cleaned with 70% ethanol.

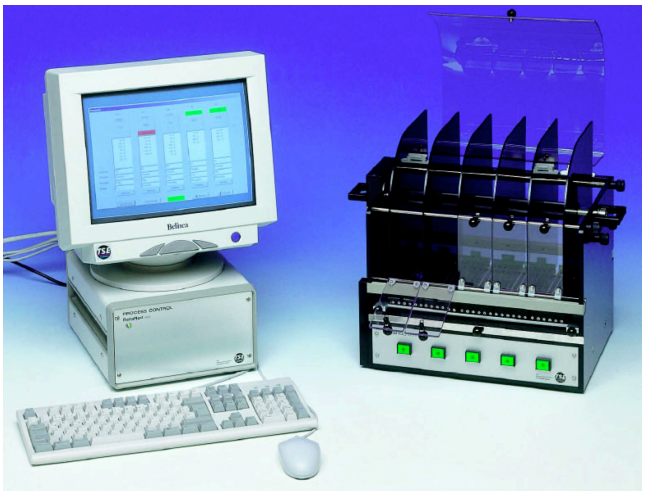

Figure 29 TSE Rota Rod apparatus for analysis motor coordination and balance and motor learning.

4.5.4. Grip test - measurement of the muscle strength

In order to elucidate the connection between nerves and muscles the grip test was used (Figure 30). A single mouse was placed on the grid. The force exerted by the animal with its limbs while it was pulled by the tail was measured. Two separate experimental sessions for front legs and all legs with three consecutive measures each were performed on a group of 31 mice (Table 3). All tested animals were weighted before the test sessions. Grip test data were analyzed using one-way ANOVA.

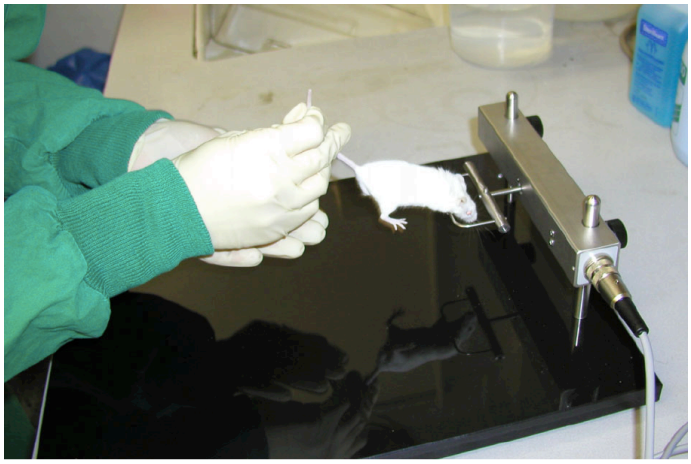

Figure 30 Apparatus for measurement of the grip strength (TSE)

4.5.5 Tail suspension test

The tail suspension test serves as a depression indicator. Mouse is subjected to the simple suspension by the tail. Initially, vigorous movements are observed in order to escape from the tail suspension, but after a few minutes the animal tends to become immobile. The tail suspension test was performed manually on 31 animals (Table 3). The mobility time recorded with a stopwatch was summed up and subtracted from the total 6 minutes observation period in order to obtain the immobility time. The cumulative immobility time is a measure of the animal's degree of helplessness ("depression"). Tail suspension data were analyzed using one-way ANOVA.

4.5.6 Operant Task- learning and memory

Animals were single-housed at least one week before the experiment and their free-feeding weights were determined. For 2 – 4 days before the test the animals were given limited amount of food to achieve body weights of approximately 85% of the initial free-feeding values.
The animals were tested in mouse operant chambers (MED-Associates, Figure 31) equipped as described (Baron and Meltzer, 2001) at the beginning of the light phase of the light/dark cycle, between 10.00 am and 8.00 pm (lights go off at 8 pm).
On the first day of the experiment, the mice were trained to drink milk from a dipper. The dipper training consisted of a single session of 60 min during which access to nose - poke holes and stimulus lights were blocked with steel panels. Dippers with milk were presented under a variable time-presentation schedule. Mice included in the studies accessed the dipper at least 20 times (dipper entries > 20). The response-acquisition sessions were conducted 24 hrs after dipper training and lasted for 90 min or until 50 correct responses were obtained. Test is carried out in complete dark. A single poke in the left hole (for one-half of the mice) and a single poke in the right hole (for the other half of the mice) resulted in turning on the light and presentation of the dipper after a 2 sec delay. The "correct" responses associated with dipper presentation are referred to as operative responses. The "incorrect" responses that did not result in dipper presentation are called inoperative responses; in addition center hole responses were counted. The time when each response occurred was recorded, allowing for the evaluation of several potential measures of learning:

-Number of operative, inoperative and center hole responses
-Percent of mice that complete 50 operative responses
-Latency to the 50^{th} operative response

-Index of curvature for 50 operative responses

A group of 20 males (WT n=7, Het n=6, KO n=7) was subjected to the operant task. Collected data were analyzed by one-way ANOVA (genotype x latency of 50 operative responses, genotype x number of operative responses, genotype x number of inoperative responses in time 90 min).

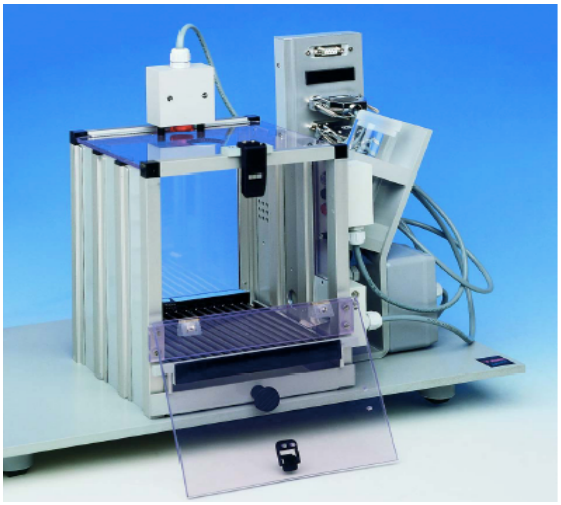

Figure 31 MED-Associate, TSE operant behavior system

5. Bibliography

Bibliography

Aszodi, A., et al. (1999). "The vasodilator-stimulated phosphoprotein (VASP) is involved in cGMP- and cAMP-mediated inhibition of agonist-induced platelet aggregation, but is dispensable for smooth muscle function." Embo J **18**(1): 37.

Bachmann, C., et al. (1999). "The EVH2 domain of the vasodilator-stimulated phosphoprotein mediates tetramerization, F-actin binding, and actin bundle formation." J Biol Chem **274**(33): 23549.

Bashaw, G. J., et al. (2000). "Repulsive axon guidance: Abelson and Enabled play opposing roles downstream of the roundabout receptor." Cell **101**(7): 703.

Bear, J. E., et al. (2000). "Negative regulation of fibroblast motility by Ena/VASP proteins." Cell **101**(7): 717.

Bear, J. E., et al. (2002). "Antagonism between Ena/VASP proteins and actin filament capping regulates fibroblast motility." Cell **109**(4): 509.

Beckerle, M. C. (1997). "Zyxin: zinc fingers at sites of cell adhesion." Bioessays **19**(11): 949.

Bentley, D. and A. Toroian-Raymond (1986). "Disoriented pathfinding by pioneer neurone growth cones deprived of filopodia by cytochalasin treatment." Nature **323**(6090): 712.

Berdiev, B. K., et al. (1996). "Regulation of epithelial sodium channels by short actin filaments." J Biol Chem **271**(30): 17704.

Bernardini, M. L., et al. (1989). "Identification of icsA, a plasmid locus of Shigella flexneri that governs bacterial intra- and intercellular spread through interaction with F-actin." Proc Natl Acad Sci U S A **86**(10): 3867.

Blasco, R., et al. (1991). "Sequence analysis, expression, and deletion of a vaccinia virus gene encoding a homolog of profilin, a eukaryotic actin-binding protein." J Virol **65**(9): 4598.

Braun, A., et al. (2002). "Genomic organization of profilin-III and evidence for a transcript expressed exclusively in testis." Gene **283**(1-2): 219.

Carlsson, L., et al. (1977). "Actin polymerizability is influenced by profilin, a low molecular weight protein in non-muscle cells." J Mol Biol **115**(3): 465.

Cooley, L., et al. (1992). "chickadee encodes a profilin required for intercellular cytoplasm transport during Drosophila oogenesis." Cell 69(1): 173.

Craig, A. M. and G. Banker (1994). "Neuronal polarity." Annu Rev Neurosci 17: 267.

Cudmore, S., et al. (1995). "Actin-based motility of vaccinia virus." Nature 378(6557): 636.

Damke, H., et al. (1994). "Induction of mutant dynamin specifically blocks endocytic coated vesicle formation." J Cell Biol 127(4): 915.

Di Monte, D., et al. (1984). "Menadione-induced cytotoxicity is associated with protein thiol oxidation and alteration in intracellular Ca2+ homeostasis." Arch Biochem Biophys 235(2): 343.

Di Nardo, A., et al. (2000). "Alternative splicing of the mouse profilin II gene generates functionally different profilin isoforms." J Cell Sci 113 Pt 21: 3795.

Di Nardo, A., et al. (2000). "Alternative splicing of the mouse profilin II gene generates functionally different profilin isoforms." J Cell Sci 113 Pt 21(7): 3795.

Fan, J. and J. A. Raper (1995). "Localized collapsing cues can steer growth cones without inducing their full collapse." Neuron 14(2): 263.

Furukawa, K., et al. (1997). "The actin-severing protein gelsolin modulates calcium channel and NMDA receptor activities and vulnerability to excitotoxicity in hippocampal neurons." J Neurosci 17(21): 8178.

Gertler, F. B., et al. (1990). "Genetic suppression of mutations in the Drosophila abl proto-oncogene homolog." Science 248(4957): 857.

Gertler, F. B., et al. (1996). "Mena, a relative of VASP and Drosophila Enabled, is implicated in the control of microfilament dynamics." Cell 87(2): 227.

Gieselmann, R., et al. (1995). "Distinct biochemical characteristics of the two human profilin isoforms." Eur J Biochem 229(3): 621.

Giesemann, T., et al. (2003). "Complex formation between the postsynaptic scaffolding protein gephyrin, profilin, and Mena: a possible link to the microfilament system." J Neurosci 23(23): 8330.

Godenschwege, T. A., et al. (2002). "Ectopic expression in the giant fiber system of Drosophila reveals distinct roles for roundabout (Robo), Robo2, and Robo3 in dendritic guidance and synaptic connectivity." J Neurosci 22(8): 3117.

Goh, K. L., et al. (2002). "Ena/VASP proteins regulate cortical neuronal positioning." Curr Biol 12(7): 565.

Goldschmidt-Clermont, P. J., et al. (1992). "The control of actin nucleotide exchange by thymosin beta 4 and profilin. A potential regulatory mechanism for actin polymerization in cells." Mol Biol Cell 3(9): 1015.

Goldschmidt-Clermont, P. J., et al. (1991). "Regulation of phospholipase C-gamma 1 by profilin and tyrosine phosphorylation." Science 251(4998): 1231.

Grenklo, S., et al. (2003). "A crucial role for profilin-actin in the intracellular motility of Listeria monocytogenes." EMBO Rep 4(5): 523.

Haarer, B. K., et al. (1990). "Purification of profilin from Saccharomyces cerevisiae and analysis of profilin-deficient cells." J Cell Biol 110(1): 105.

Haugwitz, M., et al. (1994). "Dictyostelium amoebae that lack G-actin-sequestering profilins show defects in F-actin content, cytokinesis, and development." Cell 79(2): 303.

Honore, B., et al. (1993). "Cloning and expression of a novel human profilin variant, profilin II." FEBS Lett 330(2): 151.

Hu, E., et al. (2001). "Molecular cloning and characterization of profilin-3: a novel cytoskeleton-associated gene expressed in rat kidney and testes." Exp Nephrol 9(4): 265.

Johnson, B. D. and L. Byerly (1993). "A cytoskeletal mechanism for Ca2+ channel metabolic dependence and inactivation by intracellular Ca2+." Neuron 10(5): 797.

Kang, F., et al. (1997). "Profilin interacts with the Gly-Pro-Pro-Pro-Pro-Pro sequences of vasodilator-stimulated phosphoprotein (VASP): implications for actin-based Listeria motility." Biochemistry 36(27): 8384.

Kano, M., et al. (1992). "Synaptic excitation produces a long-lasting rebound potentiation of inhibitory synaptic signals in cerebellar Purkinje cells." Nature 356(6370): 601.

Karakesisoglou, I., et al. (1996). "Plant profilins rescue the aberrant phenotype of profilin-deficient Dictyostelium cells." Cell Motil Cytoskeleton 34(1): 36.

Karakesisoglou, I., et al. (2000). "An epidermal plakin that integrates actin and microtubule networks at cellular junctions." J Cell Biol **149**(1): 195.

Klostermann, A., et al. (2000). "The orthologous human and murine semaphorin 6A-1 proteins (SEMA6A-1/Sema6A-1) bind to the enabled/vasodilator-stimulated phosphoprotein-like protein (EVL) via a novel carboxyl-terminal zyxin-like domain." J Biol Chem **275**(50): 39647.

Ko, L., et al. (2000). "Sensitization of neuronal cells to oxidative stress with mutated human alpha-synuclein." J Neurochem **75**(6): 2546.

Krause, M., et al. (2000). "Fyn-binding protein (Fyb)/SLP-76-associated protein (SLAP), Ena/vasodilator-stimulated phosphoprotein (VASP) proteins and the Arp2/3 complex link T cell receptor (TCR) signaling to the actin cytoskeleton." J Cell Biol **149**(1): 181.

Kuge, H. and J. D. Richter (1995). "Cytoplasmic 3' poly(A) addition induces 5' cap ribose methylation: implications for translational control of maternal mRNA." Embo J **14**(24): 6301.

Kwiatkowski, D. J. and G. A. Bruns (1988). "Human profilin. Molecular cloning, sequence comparison, and chromosomal analysis." J Biol Chem **263**(12): 5910.

Lambrechts, A., et al. (1995). "Purification and characterization of bovine profilin II. Actin, poly(L-proline) and inositolphospholipid binding." Eur J Biochem **230**(1): 281.

Lambrechts, A., et al. (1997). "The mammalian profilin isoforms display complementary affinities for PIP2 and proline-rich sequences." Embo J **16**(3): 484.

Lambrechts, A. I., et al. (2000). "PKA phosphorylation of EVL, a Mena/VASP relative, regulates its interaction with actin and SH3-domains." J Biol Chem.

Lanier, L. M., et al. (1999). "Mena is required for neurulation and commissure formation." Neuron **22**(2): 313.

Lanier, L. M. and F. B. Gertler (2000). "Actin cytoskeleton: Thinking globally, actin' locally." Curr Biol **10**(18): R655.

Lassing, I. and U. Lindberg (1985). "Specific interaction between phosphatidylinositol 4,5-bisphosphate and profilactin." Nature **314**(6010): 472.

Lisberger, S. G. (1998). "Physiologic basis for motor learning in the vestibulo-ocular reflex." Otolaryngol Head Neck Surg **119**(1): 43.

Loisel, T. P., et al. (1999). "Reconstitution of actin-based motility of Listeria and Shigella using pure proteins [see comments]." Nature 401(6753): 613.

Loureiro, J. J., et al. (2002). "Critical roles of phosphorylation and actin binding motifs, but not the central proline-rich region, for Ena/vasodilator-stimulated phosphoprotein (VASP) function during cell migration." Mol Biol Cell 13(7): 2533.

Luo, L. (2000). "Rho GTPases in neuronal morphogenesis." Nat Rev Neurosci 1(3): 173.

Machesky, L. M., et al. (1994). "Purification of a cortical complex containing two unconventional actins from Acanthamoeba by affinity chromatography on profilin-agarose." J Cell Biol 127(1): 107.

Machesky, L. M., et al. (1994). "Vaccinia virus expresses a novel profilin with a higher affinity for polyphosphoinositides than actin." Biochemistry 33(35): 10815.

Machesky, L. M., et al. (1997). "Mammalian actin-related protein 2/3 complex localizes to regions of lamellipodial protrusion and is composed of evolutionarily conserved proteins." Biochem J 328 (Pt 1): 105.

Mammoto, A., et al. (1998). "Interactions of drebrin and gephyrin with profilin." Biochem Biophys Res Commun 243(1): 86.

Manseau, L., et al. (1996). "Profilin is required for posterior patterning of the Drosophila oocyte." Development 122(7): 2109.

Marsh, L. and P. C. Letourneau (1984). "Growth of neurites without filopodial or lamellipodial activity in the presence of cytochalasin B." J Cell Biol 99(6): 2041.

Mattson, M. P. and S. W. Barger (1993). "Roles for calcium signaling in structural plasticity and pathology in the hippocampal system." Hippocampus 3 Spec No: 73.

Mauk, M. D. (1997). "Roles of cerebellar cortex and nuclei in motor learning: contradictions or clues?" Neuron 18(3): 343.

Mullins, R. D., et al. (1998). "The interaction of Arp2/3 complex with actin: nucleation, high affinity pointed end capping, and formation of branching networks of filaments." Proc Natl Acad Sci U S A 95(11): 6181.

Nicotera, P. and S. Orrenius (1992). "Ca2+ and cell death." Ann N Y Acad Sci 648: 17.

Niebuhr, K., et al. (1997). "A novel proline-rich motif present in ActA of Listeria monocytogenes and cytoskeletal proteins is the ligand for the EVH1 domain, a protein module present in the Ena/VASP family." Embo J **16**(17): 5433.

O'Connor, T. P. and D. Bentley (1993). "Accumulation of actin in subsets of pioneer growth cone filopodia in response to neural and epithelial guidance cues in situ." J Cell Biol **123**(4): 935.

Orrenius, S., et al. (1989). "Role of Ca2+ in toxic cell killing." Trends Pharmacol Sci **10**(7): 281.

Pantaloni, D. and M. F. Carlier (1993). "How profilin promotes actin filament assembly in the presence of thymosin beta 4." Cell **75**(5): 1007.

Paulous, S., et al. (2003). "Comparison of the capacity of different viral internal ribosome entry segments to direct translation initiation in poly(A)-dependent reticulocyte lysates." Nucleic Acids Res **31**(2): 722.

Reinhard, M., et al. (1995). "The proline-rich focal adhesion and microfilament protein VASP is a ligand for profilins." Embo J **14**(8): 1583.

Rosenmund, C. and G. L. Westbrook (1993). "Calcium-induced actin depolymerization reduces NMDA channel activity." Neuron **10**(5): 805.

Rottger, S., et al. (1999). "Interactions between vaccinia virus IEV membrane proteins and their roles in IEV assembly and actin tail formation." J Virol **73**(4): 2863.

Sakurai, Y. (1990). "Hippocampal cells have behavioral correlates during the performance of an auditory working memory task in the rat." Behav Neurosci **104**(2): 253.

Schiffmann, S. N., et al. (1999). "Impaired motor coordination and Purkinje cell excitability in mice lacking calretinin." Proc Natl Acad Sci U S A **96**(9): 5257.

Schluter, K., et al. (1998). "An alpha-actinin-profilin chimaera with two alternatively operating actin-binding sites." Eur J Cell Biol **76**(1): 1.

Schubert, W. and Z. Kaprielian (2001). "Identification and characterization of a cell surface marker for embryonic rat spinal accessory motor neurons." J Comp Neurol **439**(3): 368.

Smith, F. D., et al. (1999). "Association of the D2 dopamine receptor third cytoplasmic loop with spinophilin, a protein phosphatase-1-interacting protein." J Biol Chem **274**(28): 19894.

Smith, G. A., et al. (1996). "The tandem repeat domain in the Listeria monocytogenes ActA protein controls the rate of actin-based motility, the percentage of moving bacteria, and the localization of vasodilator-stimulated phosphoprotein and profilin." J Cell Biol **135**(3): 647.

Suetsugu, S., et al. (1998). "The essential role of profilin in the assembly of actin for microspike formation." Embo J **17**(22): 6516.

Svitkina, T. M., et al. (2003). "Mechanism of filopodia initiation by reorganization of a dendritic network." J Cell Biol **160**(3): 409.

Theriot, J. A. and T. J. Mitchison (1993). "The three faces of profilin." Cell **75**(5): 835.

Thor, H., et al. (1982). "The metabolism of menadione (2-methyl-1,4-naphthoquinone) by isolated hepatocytes. A study of the implications of oxidative stress in intact cells." J Biol Chem **257**(20): 12419.

Usui, S., et al. (2003). "Synaptic targeting of PSD-Zip45 (Homer 1c) and its involvement in the synaptic accumulation of F-actin." J Biol Chem **278**(12): 10619.

Vactor, D. V., et al. (1993). "Genes that control neuromuscular specificity in Drosophila." Cell **73**(6): 1137.

Walders-Harbeck, B., et al. (2002). "The vasodilator-stimulated phosphoprotein promotes actin polymerisation through direct binding to monomeric actin." FEBS Lett **529**(2-3): 275.

Wasterlain, C. G., et al. (1993). "Pathophysiological mechanisms of brain damage from status epilepticus." Epilepsia **34 Suppl 1**: S37.

Welch, M. D., et al. (1997). "Actin polymerization is induced by Arp2/3 protein complex at the surface of Listeria monocytogenes." Nature **385**(6613): 265.

Wills, Z., et al. (1999). "Profilin and the Abl tyrosine kinase are required for motor axon outgrowth in the Drosophila embryo." Neuron **22**(2): 291.

Witke, W., et al. (1998). "In mouse brain profilin I and profilin II associate with regulators of the endocytic pathway and actin assembly." Embo J **17**(4): 967.

Witke, W., et al. (2001). "Profilin I is essential for cell survival and cell division in early mouse development." Proc Natl Acad Sci U S A **98**(7): 3832.